Journal of Pharmaceutics and Drug Research

JPDR, 2(4): 142-162
www.scitcentral.com

ISSN: 2640-6152

Review Article: Open Access

Palytoxin Time-Resolved Absorption and Resonance FT-IR and Raman Biospectroscopy and Density Functional Theory (DFT) Investigation of Vibronic-Mode Coupling Structure in Vibrational Spectra Analysis

Alireza Heidari[1,2*], Jennifer Esposito[1] and Angela Caissutti[1]

*[*1]Faculty of Chemistry, California South University, 14731 Comet St. Irvine, CA92604, USA*

[2]American International Standards Institute, Irvine, CA 3800, USA.

Received April 04, 2019; Accepted April 10, 2019; Published July 14, 2019

ABSTRACT

Palytoxin, PTX or PLTX is an intense vasoconstrictor, and is considered to be one of the most poisonous non-protein substances known, second only to maitotoxin in terms of toxicity in mice. Parameters such as FT-IR and Raman vibrational wavelengths and intensities for single crystal Palytoxin are calculated using density functional theory and were compared with empirical results. The investigation about vibrational spectrum of cycle dimers in crystal with carboxyl groups from each molecule of acid was shown that it leads to create Hydrogen bounds for adjacent molecules. The current study aimed to investigate the possibility of simulating the empirical values. Analysis of vibrational spectrum of Palytoxin is performed based on theoretical simulation and FT–IR empirical spectrum and Raman empirical spectrum using density functional theory in levels of F/6–31G*, HF/6–31++G**, MP2/6–31G, MP2/6–31++G**, BLYP/6–31G, BLYP/6–31++G**, B3LYP/6–31G and B3LYP6–31–HEG**.

Vibration modes of methylene, carboxyl acid and phenyl cycle are separately investigated. The obtained values confirm high accuracy and validity of results obtained from calculations.

Graphical abstract:

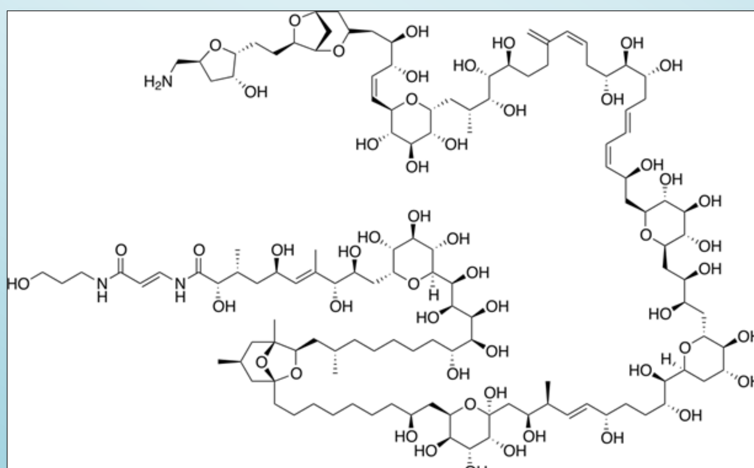

Molecular structure of Palytoxin.

Corresponding author: Alireza Heidari, Faculty of Chemistry, California South University, 14731 Comet St. Irvine, CA92604, USA, E-mail: Scholar.Researcher.Scientist@gmail.com; Alireza.Heidari@calsu.us; Central@aisi-usa.org

Citation: Heidari A, Esposito J & Caissutti A. (2019) Palytoxin Time-Resolved Absorption and Resonance FT-IR and Raman Biospectroscopy and Density Functional Theory (DFT) Investigation of Vibronic-Mode Coupling Structure in Vibrational Spectra Analysis. J Pharm Drug Res, 2(4): 142-162.

Keywords: Vibronic structure, Vibrational spectra analysis, Density functional theory (DFT), Palytoxin, Non-focal functions of Becke, Correlation functions of Lee-Yang-Parr, Time-resolved absorption and resonance, FT-IR and Raman biospectroscopy

INTRODUCTION

Palytoxin, PTX or PLTX is an intense vasoconstrictor and is considered to be one of the most poisonous non-protein substances known, second only to maitotoxin in terms of toxicity in mice [1-4]. Density Functional Theory (DFT) is one of the most powerful calculation methods for electronic structures [5-7]. Numerous results have been previously studied and indicate successful use of these methods [8-10]. The theory is one of the most appropriate methods for imulating the vibrational wavenumbers, molecular structure as well as total energy. It may be useful to initially consider the calculated results by density functional theory using F/6–31G*, HF/6–31++G**, MP2/6–31G, MP2/6–31++G**, BLYP/6–31G, BLYP/6–31++G**, B3LYP/6–31G and B3LYP6–31–HEG** approach [11-16]. It should be noted that calculations are performed by considering one degree of quantum interference as well as polarization effects of 2d orbitals in interaction [17-20].

DETAILS OF CALCULATIONS

All calculations of molecular orbital in the base of ab are performed by Gaussian 09. In calculation process, the structure of Palytoxin molecule **(Figure 1)** is optimized and FT-IR and Raman wavenumbers are calculated using F/6–31G*, HF/6–31++G**, MP2/6–31G, MP2/6– 31++G**, BLYP/6–31G, BLYP/6–31++G**, B3LYP/6–31G and B3LYP6–31–HEG** base [21-26].

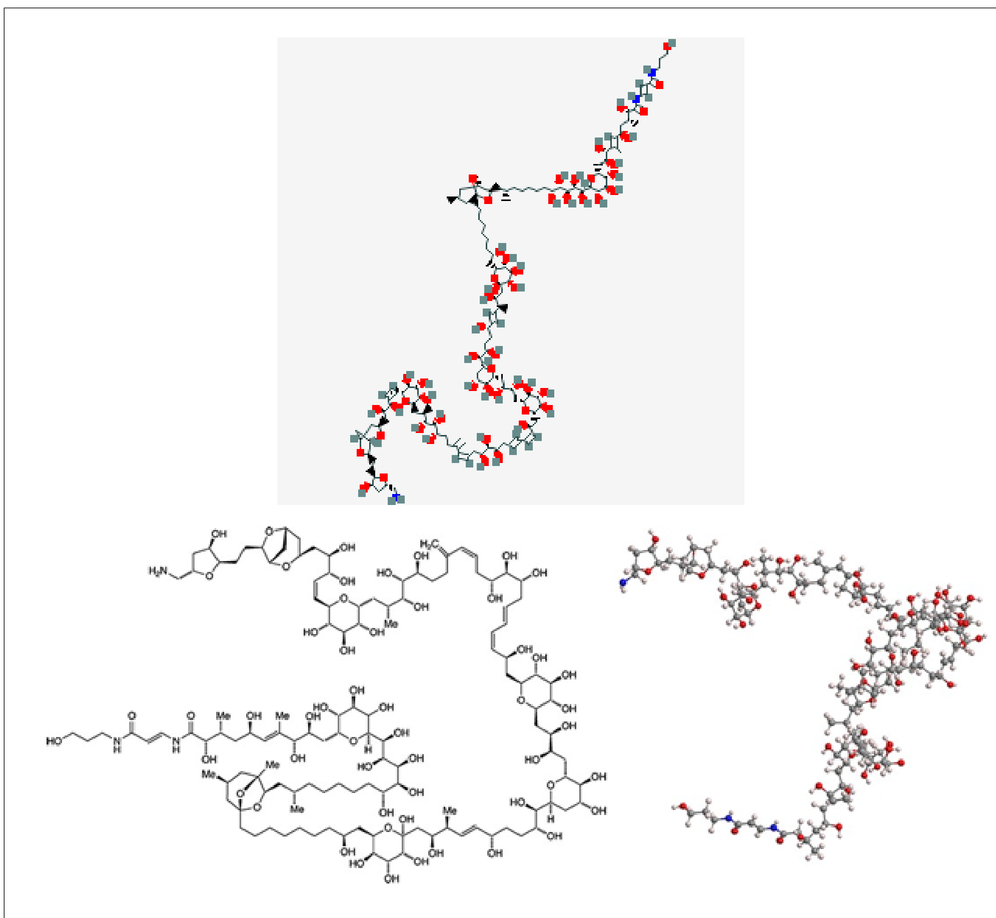

Figure 1. Different sections of the Palytoxin [52-63].

All optimized structures are adjusted with minimum energy. Harmonic vibrational wavenumbers are calculated using second degree of derivation to adjust convergence on potential surface as good as possible and to evaluate vibrational energies at zero point. In optimized structures considered in the current study, virtual frequency modes are not observed which indicates that the minimum potential energy surface is correctly chosen [27-30]. The optimized geometry is calculated by minimizing the energy relative to all geometrical quantities without forcing any constraint on molecular symmetry. Calculations were performed by Gaussian 09. The current calculation is aimed to maximize structural optimization using density functional theory [31-37]. The calculations of density functional theory is performed by F/6–31G*, HF/6–31++G**, MP2/6–31G, MP2/6– 31++G**, BLYP/6–31G, BLYP/6–31++G**, B3LYP/6–31G and B3LYP6–31–HEG** function in which non-focal functions of Becke and correlation functions of Lee-Yang-Parr beyond the Franck-Condon approximation are used. After completion of optimization process, the second order derivation of energy is calculated as a function of core coordination and is investigated to evaluate whether the structure is accurately minimized [28-43]. Vibrational frequencies used to simulate spectrums presented in the current study are derived from these second order derivatives. All calculations are performed for room temperature of 464 (K) [44-51].

VIBRATION ANALYSIS

Analysis of vibrational spectrum of Palytoxin is performed based on theoretical simulation and FT-IR empirical spectrum and Raman empirical spectrum using density functional theory in levels of F/6–31G*, HF/6–31++G**, MP2/6–31G, MP2/6–31++G**, BLYP/6–31G, BLYP/6–31++G**, B3LYP/6–31G and B3LYP6–31–HEG**. Vibration modes of methylene, carboxyl acid and phenyl cycle are separately investigated [64-77].

C–H stretching vibrations in single replacement of benzene cycles are usually seen in band range of 3265-3515 cm^{-1}. Weak Raman bands are at 3254 cm^{-1} and 3267 cm^{-1}. C–C stretching mode is a strong Raman mode at 1264 cm^{-1}. Raman weak band is seen at 1738 cm^{-1}, too. Bending mode of C–H is emerged as a weak mode at 1463 cm^{-1} and 1262 cm^{-1} and a strong band at 1346 cm^{-1} in Raman spectrum. Raman is considerably active in the range of 1265-1505 cm^{-1} which 1258 cm^{-1} indicates this issue [78-92].

C–H skew-symmetric stretching mode of methylene group is expected at 3250 cm^{-1} and its symmetric mode is expected at 3064 cm^{-1}. Skew-symmetric stretching mode of CH_2 in Palytoxin has a mode in mid-range of Raman spectrum at 3165-3285 cm^{-1}. When this mode is symmetric, it is at 3160 cm^{-1} and is sharp. The calculated wavenumbers of higher modes are at 3118 cm^{-1} and 3158 cm^{-1} for symmetric and skew–symmetric stretching mode of methylene, respectively [93-99].

Scissoring vibrations of CH_2 are usually seen at the range of 1588-1654 cm^{-1} which often includes mid-range bands. Weak bands at 1605 cm^{-1} are scissoring modes of CH_2 in Raman spectrum. Moving vibrations of methylene are usually seen at 1524 cm^{-1}. For the investigated chemical in the current study [100-107], these vibrations are at 1404 cm^{-1} were calculated using density functional theory. Twisting and rocking vibrations of CH_2 are seen in Raman spectrum at 980 cm^{-1} and 1254 cm^{-1}, respectively, which are in good accordance with the results at 964 cm^{-1} and 1219 cm^{-1}, respectively [108-121].

In a non-ionized carboxyl group (COOH), stretching vibrations of carbonyl (C=O) are mainly observed at the range of 1905-1953 cm^{-1}. If dimer is considered as an intact constituent, two stretching vibrations of carbonyl for symmetric stretching are at 1805-1850 cm^{-1} in Raman spectrum. In the current paper, stretching vibration of carbonyl mode is at 1863 cm^{-1} which is a mid-range value [122-137].

Stretching and bending bands of hydroxyl can be identified by width and band intensity which in turn is dependent on bond length of Hydrogen. In dimer form of Hydrogen bond, stretching band of O–H is of a strong Raman peak at 1436 cm^{-1} which is due to in-plain metamorphosis mode [138-179]. Out-of-plain mode of O–H group is a very strong mode of peak at 1114 cm^{-1} of Raman spectrum. The stretching mode of C–O (H) emerges as a mid-band of Raman spectrum at 1312 cm^{-1} [180-211].

Lattice vibrations are usually seen at the range of 0-615 cm^{-1}. These modes are induced by rotary and transferring vibrations of molecules and vibrations and are including Hydrogen bond [212-243]. Bands with low wavenumbers of Hydrogen bond vibrations in FT-IR and Raman spectrum **(Figure 2)** are frequently weak, width and unsymmetrical . Rotary lattice vibrations are frequently stronger than transferring ones. Intra-molecular vibrations with low wavenumbers involving two-bands O–H…O dimer at 153 cm^{-1}, 263 cm^{-1} and 314 cm^{-1} are attributed to a rotary moving of two molecules involving in-plain rotation of molecules against each other [244-267].

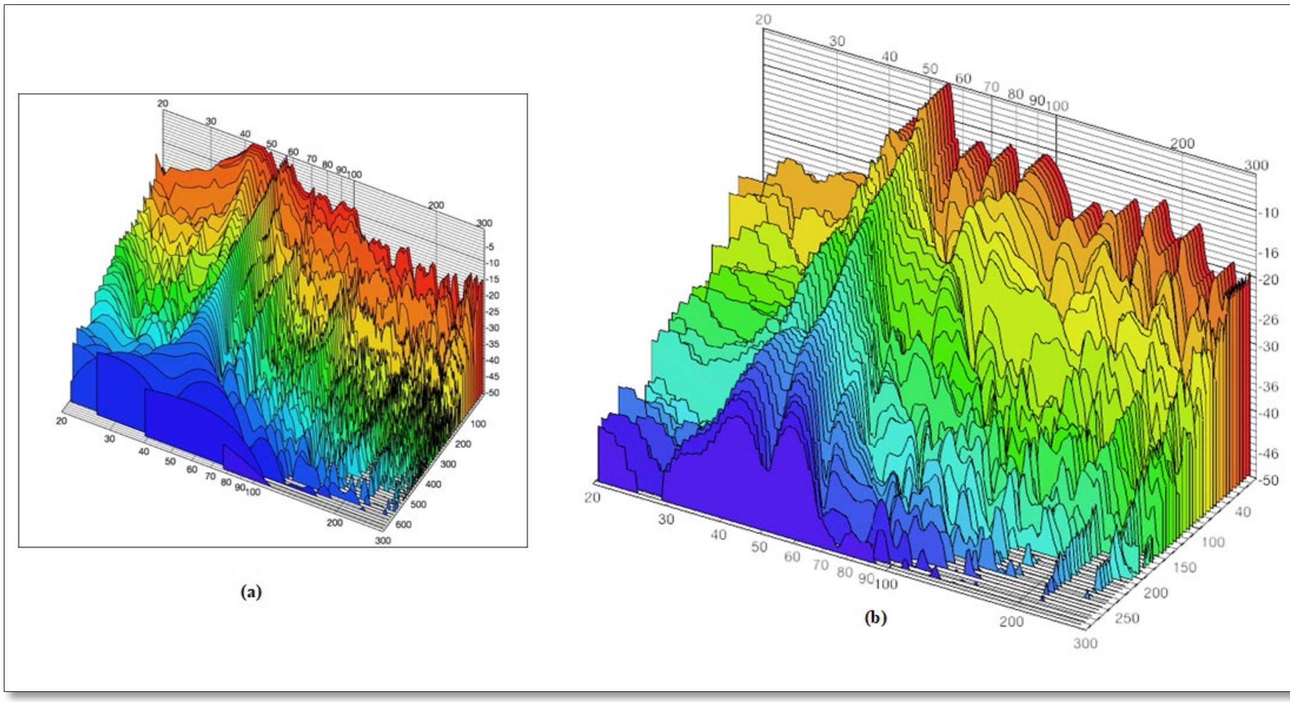

Figure 2. 3D simulation of (a) FT-IR spectrum and (b) Raman spectrum of Palytoxin.

CONCLUSION AND SUMMARY

Calculations of density functional theory using F/6–31G*, HF/6–31++G**, MP2/6–31G, MP2/6–31++G**, BLYP/6–31G, BLYP/6–31++G**, B3LYP/6–31G and B3LYP6–31–HEG** levels were used to obtain vibrational wavenumbers and intensities in single crystal of Palytoxin [268-293].

Investigation and consideration of vibrational spectrum confirm the formation of dimer cycles in the investigated crystal with carboxyl groups from each Hydrogen molecule of acid protected from adjacent molecules [294-309]. The calculated vibrational spectrum which obtains from calculations of density functional theory is in good accordance with recorded empirical values which indicates successful simulation of the problem. The obtained results indicate that the results obtained from theoretical calculations are valid through comparing with empirical recorded results [310-319].

ACKNOWLEDGEMENT

Authors are supported by an American International Standards Institute (AISI) Future Fellowship Grant FT1201009373521. We acknowledge Ms. Isabelle Villena for instrumental support and Dr. Michael N Cocchi for constructing graphical abstract figure. We gratefully acknowledge Prof. Dr. Christopher Brown for proof reading the manuscript.

REFERENCES

1. Yu P, Wu J, Liu S, Xiong J, Jagadish C, et al. (2016) Design and fabrication of silicon nanowires towards efficient solar cells. Nano Today 11: 704-737.
2. Sandhu S, Fan S (2015) Current-voltage enhancement of a single coaxial nanowire solar cell. ACS Photonics 2: 1698-1704.
3. van Dam D, Van Hoof NJJ, Cui Y, van Veldhoven PJ, Bakkers EPAM, et al. (2016) High-efficiency nanowire solar cells with omni-directionally enhanced absorption due to self-aligned indium-tin-oxide mie scatterers. ACS Nano 10: 11414-11419.
4. Luo S, Yu WB, He Y, Ouyang G (2015) Size-dependent optical absorption modulation of Si/Ge and Ge/Si core/shell nanowires with different cross-sectional geometries. Nanotechnology 26: 085702.
5. Yu P, Yao Y, Wu J, Niu X, Rogach AL, et al. (2017) Effects of plasmonic metal core-dielectric shell nanoparticles on the broadband light absorption enhancement in thin film solar cells. Sci Rep 7: 7696.
6. Gouda AM, Allam NK, Swillam MA (2017) Efficient fabrication methodology of wide angle black silicon for energy harvesting applications. RSC Adv 7: 26974-26982.
7. Branz HM, Yost VE, Ward S, Jones KM, To B, et al. (2009) Nanostructured black silicon and the optical

reflectance of graded-density surfaces. Appl Phys Lett 94: 231121.

8. Fazio B, Artoni P, Antonía Iatí M, D'Andrea C, Lo Faro MJ, et al. (2016) Strongly enhanced light trapping in a two-dimensional silicon nanowire random fractal array. Light Sci Appl 5: e16062.
9. Ko MD, Rim T, Kim K, Meyyappan M, Baek CK (2015) High efficiency silicon solar cell based on asymmetric nanowire. Sci Rep 5: 11646.
10. Oh J, Yuan HC, Branz HM (2012) An 18.2% efficient black-silicon solar cell achieved through control of carrier recombination in nanostructures. Nat Nanotechnol 7: 743-748.
11. Lin H, Xiu F, Fang M, Yip S, Cheung HY, et al. (2014) Rational design of inverted nanopencil arrays for cost-effective, broadband and omnidirectional light harvesting. ACS Nano 8: 3752-3760.
12. Garnett E, Yang P (2010) Light trapping in silicon nanowire solar cells. Nano Lett 10: 1082-1087.
13. Misra S, Yu L, Foldyna M, Roca I, Cabarrocas P (2013) High efficiency and stable hydrogenated amorphous silicon radial junction solar cells built on VLS-grown silicon nanowires. Sol Energy Mater Sol Cells 118: 90-95.
14. Kelzenberg MD, Boettcher SW, Petykiewicz JA, Turner-Evans DB, Putnam MC, et al. (2010) Enhanced absorption and carrier collection in Si wire arrays for photovoltaic applications. Nat Mater 9: 239-244.
15. Tian B, Zheng X, Kempa TJ, Fang Y, Yu N, et al. (2007) Coaxial silicon nanowires as solar cells and nanoelectronic power sources. Nature 449: 885-889.
16. Razek SA, Swillam MA, Allam NK (2014) Vertically aligned crystalline silicon nanowires with controlled diameters for energy conversion applications: Experimental and theoretical insights. J Appl Phys 115: 194305.
17. Dhindsa N, Walia J, Saini SSA (2016) Platform for colorful solar cells with enhanced absorption. Nanotechnology 27: 495203.
18. Dhindsa N, Walia J, Pathirane M, Khodadad I, Wong WS, et al. (2016) Adjustable optical response of amorphous silicon nanowires integrated with thin films. Nanotechnology 27: 145703.
19. Zhu J, Yu Z, Burkhard GF, Hsu CM, Connor ST, et al. (2009) Optical absorption enhancement in amorphous silicon nanowire and nanocone arrays. Nano Lett 9: 279-282.
20. Klinger D, Łusakowska E, Zymierska D (2006) Nano-structure formed by nanosecond laser annealing on amorphous Si surface. Mater Sci Semicond Process 9: 323-326.
21. Kumar P, Krishna MG, Bhattacharya A (2009) Excimer laser induced nanostructuring of silicon surfaces. J Nanosci Nanotechnol 9: 3224-3232.
22. Kumar P (2010) Surface modulation of silicon surface by excimer laser at laser fluence below ablation threshold. Appl Phys A Mater Sci Process 99: 245-250.
23. Adikaari AADT, Silva SRP (2005) Thickness Dependence of properties of excimer laser crystallized nano-polycrystalline silicon. J Appl Phys 97: 114305.
24. Adikaari AADT, Dissanayake DMNM, Hatton RA, Silva SRP (2007) Efficient laser textured nanocrystalline silicon-polymer bilayer solar cells. Appl Phys Lett 90: 203514.
25. Adikaari AADT, Silva SRP (2008) Excimer laser crystallization and nanostructuring of amorphous silicon for photovoltaic applications. Nano 3: 117-126.
26. Tang YF, Silva SRP, Boskovic BO, Shannon JM, Rose MJ (2002) Electron field emission from excimer laser crystallized amorphous silicon. Appl Phys Lett 80: 4154-4156.
27. Jin S, Hong S, Mativenga M, Kim B, Shin HH, et al. (2016) Low temperature polycrystalline silicon with single orientation on glass by blue laser annealing. Thin Solid Films 616: 838-841.
28. Crouch CH, Carey JE, Warrender JM, Aziz MJ, Mazur E, et al. (2004) Comparison of structure and properties of femtosecond and nanosecond laser-structured silicon. Appl Phys Lett 84: 1850-1852.
29. Wu C, Crouch CH, Zhao L, Carey JE, Younkin R, et al. (2001) Near-unity below-band-gap absorption by microstructured silicon. Appl Phys Lett 78: 1850-1852.
30. Pedraza AJ, Fowlkes JD, Lowndes DH (1999) Silicon microcolumn arrays grown by nanosecond pulsed-excimer laser irradiation. Appl Phys Lett 74: 2322.
31. Pedraza AJ, Fowlkes JD, Mao C, Jesse S, Lowndes DH (2000) Surface micro-structuring of silicon by excimer-laser irradiation in reactive atmospheres. Appl Surf Sci 168: 251-257.
32. Porte HP, Turchinovich D, Persheyev S, Fan Y, Rose MJ, et al. (2013) On ultrafast photoconductivity dynamics and crystallinity of black silicon. IEEE Trans Terahertz Sci Technol 3: 331-341.
33. Georgiev DG, Baird RJ, Avrutsky I, Auner G, Newaz G (2004) controllable excimer-laser fabrication of conical nano-tips on silicon thin films. Appl Phys Lett 84: 4881-4883.

34. Eizenkop J, Avrutsky I, Georgiev DG, Chaudchary V (2008) Single-pulse excimer laser nanostructuring of silicon: A heat transfer problem and surface morphology. J Appl Phys 103: 094311.
35. Eizenkop J, Avrutsky I, Auner G, Georgiev DG, Chaudhary V (2007) Single pulse excimer laser nanostructuring of thin silicon films: Nanosharp cones formation and a heat transfer problem. J Appl Phys 101: 094301.
36. Hong L, Wang XC, Zheng HY, He L, Wang H, et al. (2013) Femtosecond laser induced nanocone structure and simultaneous crystallization of 1.6 μM amorphous silicon thin film for photovoltaic application. J Phys D Appl. Phys 46: 195109.
37. Hong L, Wang X, Rusli, Wang H, Zheng H, et al. (2012) Crystallization and surface texturing of amorphous-Si induced by UV laser for photovoltaic application. J Appl Phys 111: 043106.
38. Magdi S, Swillam MA (2017) Broadband absorption enhancement in amorphous Si solar cells using metal gratings and surface texturing. Proc SPIE 10099: 1009912.
39. Diedenhofen SL, Janssen OTA, Grzela G, Bakkers EPAM, Gómez Rivas J (2011) Strong geometrical dependence of the absorption of light in arrays of semiconductor nanowires. ACS Nano 5: 2316-2323.
40. Jäger ST, Strehle S (2014) Design parameters for enhanced photon absorption in vertically aligned silicon nanowire arrays. Nanoscale Res Lett 9: 511.
41. Gouda AM, Elsayed MY, Khalifa AE, Ismail Y, Swillam MA (2016) Lithography-free wide-angle antireflective self-cleaning silicon nanocones. Opt Lett 41: 3575.
42. Magdi S, Swillam MA (2017) Optical analysis of Si-tapered nanowires/low band gap polymer hybrid solar cells. Proc SPIE 10099: 100991D.
43. Jiang Y, Gong X, Qin R, Liu H, Xia C, et al. (2016) Efficiency enhancement mechanism for Poly(3, 4-ethylenedioxythiophene) Poly(styrenesulfonate)/silicon nanowires hybrid solar cells using alkali treatment. Nanoscale Res Lett 11: 267.
44. Gong X, Jiang Y, Li M, Liu H, Ma H (2015) Hybrid tapered silicon nanowire/PEDOT:PSS solar cells. RSC Adv 5: 10310-10317.
45. Mohammad NS (2014) Understanding quantum confinement in nanowires: Basics, applications and possible laws. J Phys Condens Matter 26: 423202.
46. Zhang A, Luo S, Ouyang G, Yang GW (2013) Strain-induced optical absorption properties of semiconductor nanocrystals. J Chem Phys 138: 244702.
47. He Y, Yu W, Ouyang G (2016) Shape-dependent conversion efficiency of Si nanowire solar cells with polygonal cross-sections. J Appl Phys 119: 225101.
48. Tchakarov S, Das D, Saadane O, Kharchenko AV, Suendo V, et al. (2004) Helium versus hydrogen dilution in the optimization of polymorphous silicon solar cells. J Non-Cryst Solids 338-340: 668-672.
49. Roszairi H, Rahman S (2002) High deposition rate thin film hydrogenated amorphous silicon prepared by D.C. plasma enhanced chemical vapor deposition of helium diluted silane. IEEE International Conference on Semiconductor Electronics Proceedings. ICSE Panang, Malaysia, IEEE: New York, NY USA, pp: 300-303.
50. N'Guyen TTT, Duong HTT, Basuki J, Montembault V, Pascual S et al. (2013) Functional iron oxide magnetic nanoparticles with hyperthermia-induced drug release ability by using a combination of orthogonal click reactions. Angew Chem Int Ed 52: 14152-14156.
51. Xu Z, Zhao Y, Wang X, Lin TA (2013) Thermally healable polyhedral oligomeric silsesquioxane (POSS) nanocomposite based on Diels-Alder chemistry. Chem Commun 49: 6755-6757.
52. Engel T, Kickelbick G (2014) Self-healing nanocomposites from silica – polymer core – shell nanoparticles. Polym Int 63: 915-923.
53. Engel T, Kickelbick G (2015) Furan-modified spherosilicates as building blocks for self- healing materials. Eur J Inorg Chem, pp: 1226-1232.
54. Torres-Lugo M, Rinaldi C (2013) Thermal potentiation of chemotherapy by magnetic nanoparticles. Nanomedicine 8: 1689-1707.
55. Hohlbein N, Shaaban A, Bras AR, Pyckhout-Hintzen W, Schmidt AM (2015) Self-healing dynamic bond-based rubbers: understanding the mechanisms in ionomeric elastomer model systems. Chem Phys 17: 21005-21017.
56. Wu CS, Kao TH, Li HY, Liu YL (2012) Preparation of polybenzoxazine-functionalized Fe3O4 nanoparticles through in situ Diels-Alder polymerization for high performance magnetic polybenzoxazine/Fe3O4 nanocomposites. Comp Sci Technol 72: 1562-1567.
57. Menon AV, Madras G, Bose S (2018) Ultrafast self-healable interfaces in polyurethane nanocomposites designed using Diels-Alder "Click" as an efficient microwave absorber. ACS Omega 3: 1137-1146.
58. Engel T, Kickelbick G (2013) Thermoreversible reactions on inorganic nanoparticle surfaces: Diels-Alder reactions on sterically crowded surfaces. Chem Mater 25: 149-157.

59. Schäfer S, Kickelbick G (2015) Self-healing polymer nanocomposites based on Diels-Alder reactions with silica nanoparticles: The role of the polymer matrix. Polymer 69: 357-368.

60. Park JS, Darlington T, Starr AF, Takahashi K, Riendeau J, et al. (2010) Multiple healing effect of thermally activated self-healing composites based on Diels-Alder reaction. Comp Sci Technol 70: 2154-2159.

61. Li J, Liang J, Li L, Ren F, Hu W, et al. (2014) Healable capacitive touch screen sensors based on transparent composite electrodes comprising silver nanowires and a furan/maleimide Diels-Alder cycloaddition polymer ACS Nano 8: 12874-12882.

62. Sun S, Zeng H, Robinson DB, Raoux S, Rice PM, et al. (2004) Monodisperse MFe2O4 (M=Fe, Co, Mn) nanoparticles. J Am Chem Soc 126: 273-279.

63. Frison R, Cernuto G, Cervellino A, Zaharko O, Colonna GM, et al. (2013) Magnetite-maghemite nanoparticles in the 5-15 nm range: Correlating the core-shell composition and the surface structure to the magnetic properties: A total scattering study Chem Mater 25: 4820-4827.

64. Santoyo Salazar J, Perez L, de Abril O, Truong Phuoc L, Ihiawakrim D, et al. (2011) Magnetic iron oxide nanoparticles in 10-40 nm range: Composition in terms of magnetite/maghemite ratio and effect on the magnetic properties. Chem Mater 23: 1379-1386.

65. Guerrero G, Mutin PH, Vioux A (2001) Anchoring of Phosphonate and phosphinate coupling molecules on titania particles. Chem Mater 13: 4367-4373.

66. Babu K, Dhamodharan R (2008) Grafting of Poly(methyl methacrylate) brushes from magnetite nanoparticles using a phosphonic acid based initiator by ambient temperature atom transfer radical polymerization (ATATRP). Nanoscale Res Lett 3: 109-117.

67. Mohapatra S, Pramanik P (2009) Synthesis and stability of functionalized iron oxide nanoparticles using organophosphorus coupling agents. Colloids Surf A 339: 35-42.

68. Larsen BA, Hurst KM, Ashurst WR, Serkova NJ, Stoldt CR (2012) Mono- and di-alkoxysilane surface modification of super paramagnetic iron oxide nanoparticles for application as magnetic resonance imaging contrast agents. J Mater Res 27: 1846-1852.

69. Davis K, Qi B, Witmer M, Kitchens CL, Powell BA, et al. (2014) Quantitative measurement of ligand exchange on iron oxides via radiolabeled oleic acid. Langmuir 30: 10918-10925.

70. Feichtenschlager B, Pabisch S, Peterlik H, Kickelbick G (2012) Nanoparticle assemblies as probes for self-assembled monolayer characterization: Correlation between surface functionalization and agglomeration behavior. Langmuir 28: 741-750.

71. Musa OM (2016) Handbook of Maleic Anhydride Based Materials: Syntheses, Properties and Applications. Springer International Publishing: Switzerland, p: 175ff.

72. Sauer R, Froimowicz P, Scholler K, Cramer JM, Ritz S, et al. (2012) Design, synthesis and mini-emulsion polymerization of new phosphonate surfmers and application studies of the resulting nanoparticles as model systems for biomimetic mineralization and cellular uptake. Chem Eur J 18: 5201-5212.

73. Lu C, Bhatt LR, Jun HY, Park SH, Chai KY (2012) Carboxyl-polyethylene glycol-phosphoric acid: A ligand for highly stabilized iron oxide nanoparticles. J Mater Chem 22: 19806-19811.

74. Patsula V, Kosinova L, Lovric M, Ferhatovic Hamzic L, Rabyk M, et al. (2016) Super paramagnetic Fe3O4 nanoparticles: Synthesis by thermal decomposition of iron(III) glucuronate and application in magnetic resonance imaging. ACS Appl Mater Interfaces 8: 7238-7247.

75. Pothayee N, Balasubramaniam S, Davis RM, Riffle JS, Carroll MRJ, et al. (2011) Synthesis of 'ready-to-adsorb' polymeric nanoshells for magnetic iron oxide nanoparticles via atom transfer radical polymerization. Polymer 52: 1356-1366.

76. Daou J, Begin-Colin S, Grenèche JM, Thomas F, Derory A, et al. (2007) Phosphate adsorption properties of magnetite-based nanoparticles. Chem Mater 19: 4494-4505.

77. Breucker L, Landfester K, Taden A (2015) Phosphonic acid-functionalized polyurethane dispersions with improved adhesion properties. ACS Appl Mater Interfaces 7: 24641-24648.

78. Sahoo Y, Pizem H, Fried T, Golodnitsky D, Burstein L, et al. (2001) Alkyl phosphonate/phosphate coating on magnetite nanoparticles: A comparison with fatty acids. Langmuir 17: 7907-7911.

79. Longo RC, Cho K, Schmidt WG, Chabal YJ, Thissen P, et al. (2013) Monolayer doping via phosphonic acid grafting on silicon: Microscopic Insight from infrared spectroscopy and density functional theory calculations. Adv Funct Mater 23: 3471-3477.

80. Luschtinetz R, Seifert G, Jaehne E, Adler HJP (2007) Infrared spectra of alkyl phosphonic acid bound to aluminum surfaces. Macromol Symp 254: 248-253.

81. Thomas LC, Chittenden RA (1964) Characteristic infrared absorption frequencies of organophosphorus compounds-II P-O-(X) bonds. Spectrochim Acta 20: 489-502.

82. Quinones R, Shoup D, Behnke G, Peck C, Agarwal S, et al. (2017) Study of perfluorophosphonic acid surface modifications on zinc oxide nanoparticles. Materials 10: 1-16.

83. Lalatonne Y, Paris C, Serfaty JM, Weinmann P, Lecouvey M, et al. (2008) Bis-phosphonates-ultra small superparamagnetic iron oxide nanoparticles: A platform towards diagnosis and therapy. Chem Commun, pp: 2553-2555.

84. Jastrzebski W, Sitarz M, Rokita M, Bulat K (2011) Infrared spectroscopy of different phosphates structures. Spectrochim Acta Part A 79: 722-727.

85. Brodard-Severac F, Guerrero G, Maquet J, Florian P, Gervais C, et al. (2008) High-field 17O MAS NMR investigation of phosphonic acid monolayers on titania. Chem Mater 20: 5191-5196.

86. Brice-Profeta S, Arrio MA, Tronc E, Menguy N, Letard I, et al. (2005) Magnetic order in g-Fe2O3 nanoparticles: A XMCD study. J Magn Magn Mater 288: 354-365.

87. Tronc E, Ezzir A, Cherkaoui R, Chanéac C, Noguès M, et al. (2000) Surface-related properties of g-Fe2O3 Nanoparticles. J Magn Magn Mater 221: 63-79.

88. Yee C, Kataby G, Ulman A, Prozorov T, White H, et al. (1999) Self-assembled monolayers of alkane-sulfonic and -phosphonic acids on amorphous iron oxide nanoparticles. Langmuir 15: 7111-7115.

89. Jolivet JP, Chaneac C, Tronc E (2004) Iron oxide chemistry from molecular clusters to extended solid networks. Chem Commun, pp: 481-487.

90. Campbell VE, Tonelli M, Cimatti I, Moussy JB, Tortech L, et al. (2016) Engineering the magnetic coupling and anisotropy at the molecule-magnetic surface interface in molecular spintronic devices. Nat Commun 7: 13646.

91. Pabisiak T, Winiarski MJ, Ossowski T, Kiejna A (2016) Adsorption of gold sub nano-structures on a magnetite (111) surface and their interaction with CO. Phys Chem Chem Phys 18: 18169-18179.

92. Gomes R, Hassinen A, Szczygiel A, Zhao Q, Vantomme A, et al. (2011) Binding of phosphonic acids to CdSe quantum dots: A solution NMR study J Phys Chem Lett 2: 145-152.

93. Chun YJ, Park JN, Oh GM, Hong SI, Kim YJ (1994) Synthesis of ω-Phthalimidoalkylphosphonates synthesis 1994: 909-910.

94. Heidari A, Brown C (2015) Study of composition and morphology of cadmium oxide (CdO) nanoparticles for eliminating cancer cells. J Nanomed Res 2: 20.

95. Heidari A, Brown C (2015) Study of surface morphological, phytochemical and structural characteristics of rhodium (III) oxide (Rh2O3) nanoparticles. Int J Pharmacol Phytochem Ethnomed 1: 15-19.

96. Heidari A (2016) An experimental biospectroscopic study on seminal plasma in determination of semen quality for evaluation of male infertility. Int J Adv Technol 7: e007.

97. Heidari A (2016) Extraction and pre-concentration of N–Tolyl–Sulfonyl–Phosphoramid–Saeure–Dichlorid as an anti-cancer drug from plants: A pharmacognosy study. J Pharmacogn Nat Prod 2: e103.

98. Heidari A (2016) A thermodynamic study on hydration and dehydration of DNA and RNA − Amphiphile complexes. J Bioeng Biomed Sci S: 006.

99. Heidari A (2016) Computational studies on molecular structures and carbonyl and ketene groups' effects of singlet and triplet energies of azidoketene O=C=CH–NNN and isocyanatoketene O=C=CH–N=C=O. J Appl Comp Math 5: e142.

100. Heidari A (2016) Study of irradiations to enhance the induces the dissociation of hydrogen bonds between peptide chains and transition from helix structure to random coil structure using ATR-FTIR, Raman and 1HNMR Spectroscopies. J Biomol Res Ther 5: e146.

101. Heidari A (2016) Future prospects of point fluorescence spectroscopy, fluorescence imaging and fluorescence endoscopy in photodynamic therapy (PDT) for cancer cells. J Bioanal Biomed 8: e135.

102. Heidari A (2016) A bio-spectroscopic study of DNA density and color role as determining factor for absorbed irradiation in cancer cells. Adv Cancer Prev 1: e102.

103. Heidari A (2016) Manufacturing process of solar cells using cadmium oxide (CdO) and rhodium (III) oxide (Rh_2O_3) nanoparticles. J Biotechnol Biomater 6: e125.

104. Heidari A (2016) A novel experimental and computational approach to photobiosimulation of telomeric DNA/RNA: A biospectroscopic and photobiological study. J Res Dev 4: 144.

105. Heidari A (2016) Biochemical and pharmacodynamical study of microporous molecularly imprinted polymer selective for vancomycin, teicoplanin, oritavancin, telavancin and dalbavancin binding. Biochem Physiol 5: e146.

106. Heidari A (2016) Anti-cancer effect of UV irradiation at presence of cadmium oxide (CdO) nanoparticles on DNA of cancer cells: A photodynamic therapy study. Arch Cancer Res 4: 1.

107. Heidari A (2016) Biospectroscopic study on multi–component reactions (MCRs) in two: A-Type and B-Type conformations of nucleic acids to determine ligand binding modes. Binding constant and stability of nucleic acids in cadmium oxide (CdO) nanoparticles-nucleic acids complexes as anti-cancer drugs. Arch Cancer Res 4: 2.

108. Heidari A (2016) Simulation of temperature distribution of DNA/RNA of human cancer cells using time-dependent bio-heat equation and Nd: YAG lasers. Arch Cancer Res 4: 2.

109. Heidari A (2016) Quantitative structure-activity relationship (QSAR) approximation for cadmium oxide (CdO) and rhodium (iii) oxide (Rh2O3) nanoparticles as anti-cancer drugs for the catalytic formation of proviral DNA from viral RNA using multiple linear and non-linear correlation approach. Ann Clin Lab Res 4: 1.

110. Heidari A (2016) Biomedical study of cancer cells DNA therapy using laser irradiations at presence of intelligent nanoparticles. J Biomedical Sci 5: 2.

111. Heidari A (2016) Measurement the amount of vitamin D2 (ergocalciferol), vitamin D3 (cholecalciferol) and absorbable calcium (Ca2+), iron (II) (Fe2+), magnesium (Mg2+), phosphate (PO4-) and zinc (Zn2+) in apricot using high–performance liquid chromatography (HPLC) and spectroscopic techniques. J Biom Biostat 7: 292.

112. Heidari A (2016) Spectroscopy and quantum mechanics of the helium dimer (He2+), neon dimer (Ne2+), argon dimer (Ar2+), krypton dimer (Kr2+), xenon dimer (Xe2+), radon dimer (Rn2+) and ununoctium dimer (Uuo2+) molecular cations. Chem Sci J 7: e112.

113. Heidari A (2016) Human toxicity photodynamic therapy studies on DNA/RNA complexes as a promising new sensitizer for the treatment of malignant tumors using bio-spectroscopic techniques. J Drug Metab Toxicol 7: e129.

114. Heidari A (2016) Novel and stable modifications of intelligent cadmium oxide (CdO) nanoparticles as anti-cancer drug in formation of nucleic acids complexes for human cancer cells' treatment. Biochem Pharmacol (Los Angel) 5: 207.

115. Heidari A (2016) A combined computational and QM/MM molecular dynamics study on boron nitride nanotubes (BNNTs), amorphous boron nitride nanotubes (a–BNNTs) and hexagonal boron nitride nanotubes (h–BNNTs) as hydrogen storage. Struct Chem Crystallogr Commun 2: 1.

116. Heidari A (2016) Pharmaceutical and analytical chemistry study of cadmium oxide (CdO) nanoparticles synthesis methods and properties as anti-cancer drug and its effect on human cancer cells. Pharm Anal Chem Open Access 2: 113.

117. Heidari A (2016) A chemotherapeutic and biospectroscopic investigation of the interaction of double-standard DNA/RNA-binding molecules with cadmium oxide (CdO) and rhodium (III) oxide (Rh2O3) nanoparticles as anti–cancer drugs for cancer cells' treatment. Chemo Open Access 5: e129.

118. Heidari A (2016) Pharmacokinetics and experimental therapeutic study of DNA and other biomolecules using lasers: Advantages and applications. J Pharmacokinet Exp Ther 1: e005.

119. Heidari A (2016) Determination of ratio and stability constant of DNA/RNA in human cancer cells and cadmium oxide (CdO) nanoparticles complexes using analytical electrochemical and spectroscopic techniques. Insights Anal Electrochem 2: 1.

120. Heidari A (2016) Discriminate between antibacterial and non-antibacterial drugs artificial neutral networks of a multilayer perceptron (MLP) type using a set of topological descriptors. J Heavy Met Toxicity Dis 1: 2.

121. Heidari A (2016) Combined theoretical and computational study of the Belousov-Zhabotinsky chaotic reaction and Curtius rearrangement for synthesis of mechlorethamine, cisplatin, streptozotocin, cyclophosphamide, melphalan, busulphan and BCNU as anti-cancer drugs. Insights Med Phys 1: 2.

122. Heidari A (2016) A translational biomedical approach to structural arrangement of amino acids' complexes: A combined theoretical and computational study. Transl Biomed 7: 2.

123. Heidari A (2016) Ab initio and density functional theory (DFT) studies of dynamic NMR shielding tensors and vibrational frequencies of DNA/RNA and cadmium oxide (CdO) nanoparticles complexes in human cancer cells. J Nanomedine Biother Discov 6: e144.

124. Heidari A (2016) Molecular dynamics and monte–carlo simulations for replacement sugars in insulin resistance, obesity, LDL cholesterol, triglycerides, metabolic syndrome, type 2 diabetes and cardiovascular disease: A glycobiological study. J Glycobiol 5: e111.

125. Heidari A (2016) Synthesis and study of 5-[(Phenylsulfonyl)Amino]-1,3,4-Thiadiazole-2-Sulfonamide as potential anti-pertussis drug using chromatography and spectroscopy techniques. Transl Med (Sunnyvale) 6: e138.

126. Heidari A (2016) Nitrogen, oxygen, phosphorus and sulphur heterocyclic anti–cancer nano drugs separation

in the supercritical fluid of ozone (O3) using Soave-Redlich-Kwong (SRK) and Pang-Robinson (PR) equations. Electronic J Biol 12: 4.

127. Heidari A (2016) An analytical and computational infrared spectroscopic review of vibrational modes in nucleic acids. Austin J Anal Pharm Chem 3: 1058.

128. Heidari A, Brown C (2016.) Phase, composition and morphology study and analysis of Os-Pd/HfC nanocomposites. Nano Res Appl 2: 1.

129. Heidari A, Brown C (2016) Vibrational spectroscopic study of intensities and shifts of symmetric vibration modes of ozone diluted by cumene. Int J Adv Chem 4: 5-9.

130. Heidari A (2016) Study of the role of anti-cancer molecules with different sizes for decreasing corresponding bulk tumor multiple organs or tissues. Arch Can Res 4: 2.

131. Heidari A (2016) Genomics and proteomics studies of zolpidem, necopidem, alpidem, saripidem, miroprofen, zolimidine, olprinone and abafungin as anti-tumor, peptide antibiotics, antiviral and central nervous system (CNS) drugs. J Data Mining Genomics Proteomics 7: e125.

132. Heidari A (2016) Pharmacogenomics and pharmacoproteomics studies of phosphodiesterase-5 (PDE5) inhibitors and paclitaxel albumin-stabilized nanoparticles as sandwiched anti-cancer nano drugs between two DNA/RNA molecules of human cancer cells. J Pharmacogenomics Pharmacoproteomics 7: e153.

133. Heidari A (2016) Biotranslational medical and biospectroscopic studies of cadmium oxide (CdO) nanoparticles-DNA/RNA straight and cycle chain complexes as potent anti-viral, anti-tumor and anti-microbial drugs: A clinical approach. Transl Biomed 7: 2.

134. Heidari A (2016) A comparative study on simultaneous determination and separation of adsorbed cadmium oxide (CdO) nanoparticles on DNA/RNA of human cancer cells using biospectroscopic techniques and dielectrophoresis (DEP) method. Arch Can Res 4: 2.

135. Heidari A (2016) Cheminformatics and system chemistry of cisplatin, carboplatin, nedaplatin, oxaliplatin, heptaplatin and lobaplatin as anti-cancer nano drugs: A combined computational and experimental study. J Inform Data Min 1: 3.

136. Heidari A (2016) Linear and non-linear quantitative structure anti-cancer activity relationship (QSACAR) Study of hydrous ruthenium (IV) oxide (RuO2) nanoparticles as non-nucleoside reverse transcriptase inhibitors (NNRTIs) and anti-cancer nano drugs. J Integr Oncol 5: e110.

137. Heidari A (2016) Synthesis, characterization and biospectroscopic studies of cadmium oxide (CdO) nanoparticles-nucleic acids complexes absence of soluble polymer as a protective agent using nucleic acids condensation and solution reduction method. J Nanosci Curr Res 1: e101.

138. Heidari A (2016) Co-planarity and collinearity of 4'-Dinonyl–2,2'-Bithiazole in one domain of bleomycin and pingyangmycin to be responsible for binding of cadmium oxide (CdO) nanoparticles to DNA/RNA bidentate ligands as anti-tumor nano drug. Int J Drug Dev Res 8: 7-8.

139. Heidari A (2016) A pharmacovigilance study on linear and non-linear quantitative structure (chromatographic) retention relationships (QSRR) models for the prediction of retention time of anti-cancer nano drugs under synchrotron radiations. J Pharmacovigil 4: e161.

140. Heidari A (2016) Nanotechnology in preparation of semipermeable polymers. J Adv Chem Eng 6: 157.

141. Heidari A (2016) A gastrointestinal study on linear and non-linear quantitative structure (chromatographic) retention relationships (QSRR) models for analysis 5-aminosalicylates nano particles as digestive system nano drugs under synchrotron radiations. J Gastrointest Dig Syst 6: e119.

142. Heidari A (2016) DNA/RNA fragmentation and cytolysis in human cancer cells treated with diphthamide nano particles derivatives. Biomedical Data Mining 5: e102.

143. Heidari A (2016) A successful strategy for the prediction of solubility in the construction of quantitative structure-activity relationship (QSAR) and quantitative structure–property relationship (QSPR) under synchrotron radiations using genetic function approximation (GFA) algorithm. J Mol Biol Biotechnol 1: 1.

144. Heidari A (2016) Computational study on molecular structures of C20, C60, C240, C540, C960, C2160 and C3840 fullerene nano molecules under synchrotron radiations using fuzzy logic. J Material Sci Eng 5: 282.

145. Heidari A (2016) Graph theoretical analysis of zigzag polyhexamethylene biguanide, polyhexamethylene adipamide, polyhexamethylene biguanide gauze and polyhexamethylene biguanide hydrochloride (PHMB) boron nitride nanotubes (bnnts), amorphous boron nitride nanotubes (a–BNNTs) and hexagonal boron nitride nanotubes (h–BNNTs). J Appl Computat Math 5: e143.

146. Heidari A (2016) The impact of high resolution imaging on diagnosis. Int J Clin Med Imaging 3: 1000e101.

147. Heidari A (2016) A comparative study of conformational behavior of isotretinoin (13-Cis Retinoic Acid) and tretinoin (All–Trans Retinoic Acid (ATRA)) nano particles as anti-cancer nano drugs under synchrotron radiations using Hartree-Fock (HF) and density functional theory (DFT) methods. Insights Biomed 1: 2.

148. Heidari A (2016) Advances in logic, operations and computational mathematics. J Appl Computat Math 5: 5.

149. Heidari A (2016) Mathematical equations in predicting physical behavior. J Appl Computat Math 5: 5.

150. Heidari A (2016) Chemotherapy a last resort for cancer treatment. Chemo Open Access 5: 4.

151. Heidari A (2016) Separation and pre-concentration of metal cations–DNA/RNA chelates using molecular beam mass spectrometry with tunable vacuum ultraviolet (VUV) synchrotron radiation and various analytical methods. Mass Spectrom Purif Tech 2: e101.

152. Heidari A (2016) Yocto second quantitative structure-activity relationship (QSAR) and quantitative structure-property relationship (QSPR) under synchrotron radiations studies for prediction of solubility of anti-cancer nano drugs in aqueous solutions using genetic function approximation (GFA) algorithm. Insight Pharm Res 1: 1.

153. Heidari A (2016) Cancer risk prediction and assessment in human cells under synchrotron radiations using quantitative structure activity relationship (QSAR) and quantitative structure properties relationship (QSPR) studies. Int J Clin Med Imaging 3: 516.

154. Heidari A (2016) A novel approach to biology. Electronic J Biol 12: 4.

155. Heidari A (2016) Innovative biomedical equipment's for diagnosis and treatment. J Bioeng Biomed Sci 6: 2.

156. Heidari A (2016) Integrating precision cancer medicine into healthcare, medicare reimbursement changes and the practice of oncology: Trends in oncology medicine and practices. J Oncol Med Pract 1: 2.

157. Heidari A (2016) Promoting convergence in biomedical and biomaterials sciences and silk proteins for biomedical and biomaterials applications: An introduction to materials in medicine and bioengineering perspectives. J Bioeng Biomed Sci 6: 3.

158. Heidari A (2017) X-ray fluorescence and X-ray diffraction analysis on discrete element modeling of nanopowder metallurgy processes in optimal container design. J Powder Metall Min 6: 1.

159. Heidari A (2017) Biomolecular spectroscopy and dynamics of nano-sized molecules and clusters as cross-linking induced anti-cancer and immuno-oncology nano drugs delivery in DNA/RNA of human cancer cells' membranes under synchrotron radiations: A payload-based perspective. Arch Chem Res 1: 2.

160. Heidari A (2017) Deficiencies in repair of double-standard DNA/RNA-binding molecules identified in many types of solid and liquid tumors oncology in human body for advancing cancer immunotherapy using computer simulations and data analysis: Number of mutations in a synchronous tumor varies by age and type of synchronous cancer. J Appl Bioinform Comput Biol 6: 1.

161. Heidari A (2017) Electronic coupling among the five nanomolecules shuts down quantum tunneling in the presence and absence of an applied magnetic field for indication of the dimer or other provide different influences on the magnetic behavior of single molecular magnets (SMMs) as qubits for quantum computing. Glob J Res Rev 4: 2.

162. Heidari A (2017) Polymorphism in nano-sized graphene ligand-induced transformation of Au38–xAgx/xCux(SPh–tBu)24 to Au36–xAgx/xCux(SPh–tBu)24 (x=1-12) nanomolecules for synthesis of Au144–xAgx/xCux((SR)60, (SC4)60, (SC6)60, (SC12)60, (PET)60, (p–MBA)60, (F)60, (Cl)60, (Br)60, (I)60, (At)60, (Uus)60 and (SC6H13)60) nano clusters as anti-cancer nano drugs. J Nanomater Mol Nanotechnol 6: 3.

163. Heidari A (2017) Biomedical resource oncology and data mining to enable resource discovery in medical, medicinal, clinical, pharmaceutical, chemical and translational research and their applications in cancer research. Int J Biomed Data Min 6: e103.

164. Heidari A (2017) Study of synthesis, pharmacokinetics, pharmacodynamics, dosing, stability, safety and efficacy of olympiadane nanomolecules as agent for cancer enzymotherapy, immunotherapy, chemotherapy, radiotherapy, hormone therapy and targeted therapy under synchrotorn radiation. J Dev Drugs 6: e154.

165. Heidari A (2017) A novel approach to future horizon of top seven biomedical research topics to watch. In: Alzheimers, Ebola, hypersomnia, human immunodeficiency virus (HIV), tuberculosis (TB), microbiome/antibiotic resistance and endovascular stroke. J Bioeng Biomed Sci 7: e127.

166. Heidari A (2017) Opinion on computational fluid dynamics (CFD) technique. Fluid Mech Open Acc 4: 157.

167. Heidari A (2017) Concurrent diagnosis of oncology influence outcomes in emergency general surgery for

colorectal cancer and multiple sclerosis (MS) treatment using magnetic resonance imaging (MRI) and Au329(SR)84, Au329–xAgx(SR)84, Au144(SR)60, Au68(SR)36, Au30(SR)18, Au102(SPh)44, Au38(SPh)24, Au38(SC2H4Ph)24, Au21S(SAdm)15, Au36(pMBA)24 and Au25(pMBA)18 nano clusters. J Surgery Emerg Med 1: 21.

168. Heidari A (2017) Developmental cell biology in adult stem cells death and autophagy to trigger a preventive allergic reaction to common airborne allergens under synchrotron radiation using nanotechnology for therapeutic goals in particular allergy shots (Immunotherapy). Cell Biol (Henderson, NV) 6: 1.

169. Heidari A (2017) Changing metal powder characteristics for elimination of the heavy metals toxicity and diseases in disruption of extracellular matrix (ECM) proteins adjustment in cancer metastases induced by osteosarcoma, chondrosarcoma, carcinoid, carcinoma, ewing's sarcoma, fibrosarcoma and secondary hematopoietic solid or soft tissue tumors. J Powder Metall Min 6: 170.

170. Heidari A (2017) Nanomedicine-based combination anti-cancer therapy between nucleic acids and anti-cancer nano drugs in covalent nano drugs delivery systems for selective imaging and treatment of human brain tumors using hyaluronic acid, alguronic acid and sodium hyaluronate as anti-cancer nano drugs and nucleic acids delivery under synchrotron radiation. Am J Drug Deliv 5: 2.

171. Heidari A (2017) Clinical trials of dendritic cell therapies for cancer exposing vulnerabilities in human cancer cells' metabolism and metabolomics: New discoveries, unique features inform new therapeutic opportunities, biotech's bumpy road to the market and elucidating the biochemical programs that support cancer initiation and progression. J Biol Med Sci 1: e103.

172. Heidari A (2017) The design graphene-based nanosheets as a new nanomaterial in anti-cancer therapy and delivery of chemotherapeutics and biological nanodrugs for liposomal anti-cancer nano drugs and gene delivery. Br Biomed Bull 5: 305.

173. Heidari A (2017) Integrative approach to biological networks for emerging roles of proteomics, genomics and transcriptomics in the discovery and validation of human colorectal cancer biomarkers from DNA/RNA sequencing data under synchrotron radiation. Transcriptomics 5: e117.

174. Heidari A (2017) Elimination of the heavy metals toxicity and diseases in disruption of extracellular matrix (ECM) proteins and cell adhesion intelligent nanomolecules adjustment in cancer metastases using metalloenzymes and under synchrotron radiation. Lett Health Biol Sci 2: 1-4.

175. Heidari A (2017) Treatment of breast cancer brain metastases through a targeted nanomolecule drug delivery system based on dopamine functionalized multi–wall carbon nanotubes (MWCNTs) coated with nano graphene oxide (GO) and protonated polyaniline (PANI) in situ during the polymerization of aniline autogenic nanoparticles for the delivery of anti-cancer nano drugs under synchrotron radiation. Br J Res 4: 16.

176. Heidari A (2017) Sedative, analgesic and ultrasound-mediated gastrointestinal nanodrugs delivery for gastrointestinal endoscopic procedure, nanodrug-induced gastrointestinal disorders and nanodrug treatment of gastric acidity. Res Rep Gastroenterol 1: 1.

177. Heidari A (2017) Synthesis, pharmacokinetics, pharmacodynamics, dosing, stability, safety and efficacy of orphan nano drugs to treat high cholesterol and related conditions and to prevent cardiovascular disease under synchrotron radiation. J Pharm Sci Emerg Drugs 5: 1.

178. Heidari A (2017) Non-linear compact proton synchrotrons to improve human cancer cells and tissues treatments and diagnostics through particle therapy accelerators with monochromatic microbeams. J Cell Biol Mol Sci 2: 1-5.

179. Heidari A (2017) Design of targeted metal chelation therapeutics nanocapsules as colloidal carriers and blood-brain barrier (BBB) translocation to targeted deliver anti-cancer nano drugs into the human brain to treat Alzheimer's disease under synchrotron radiation. J Nanotechnol Material Sci 4: 1-5.

180. Gobato R, Heidari A (2017) Calculations using quantum chemistry for inorganic molecule simulation BeLi2SeSi. Sci J Anal Chem 5: 76-85.

181. Heidari A (2017) Different high-resolution simulations of medical, medicinal, clinical, pharmaceutical and therapeutics oncology of human lung cancer translational anti-cancer nano drugs delivery treatment process under synchrotron and x-ray radiations. J Med Oncol 1: 1.

182. Heidari A (2017) A modern ethnomedicinal technique for transformation, prevention and treatment of human malignant gliomas tumors into human benign gliomas tumors under synchrotron radiation. Am J Ethnomed 4: 1-10.

183. Heidari A (2017) Active targeted nanoparticles for anti-cancer nano drugs delivery across the blood–brain barrier for human brain cancer treatment, multiple sclerosis (MS) and Alzheimer's diseases using chemical modifications of anti-cancer nano drugs or drug–

nanoparticles through Zika virus (ZIKV) nanocarriers under synchrotron radiation. J Med Chem Toxicol 2: 1-5.

184. Heidari A (2017) Investigation of medical, medicinal, clinical and pharmaceutical applications of estradiol, mestranol (norlutin), norethindrone (NET), norethisterone acetate (NETA), norethisterone enanthate (NETE) and testosterone nanoparticles as biological imaging, cell labeling, anti-microbial agents and anti-cancer nanodrugs in nanomedicines based drug delivery systems for anti-cancer targeting and treatment. Parana J Sci Educ (PJSE) 3: 10-19.

185. Heidari A (2017) A comparative computational and experimental study on different vibrational biospectroscopy methods, techniques and applications for human cancer cells in tumor tissues simulation, modeling, research, diagnosis and treatment. Open J Anal Bioanal Chem 1: 14-20.

186. Heidari A (2017) Combination of DNA/RNA ligands and linear/non-linear visible-synchrotron radiation-driven N-doped ordered mesoporous cadmium oxide (CdO) nanoparticles photocatalysts channels resulted in an interesting synergistic effect enhancing catalytic anti-cancer activity. Enz Eng 6: 1.

187. Heidari A (2017) Modern approaches in designing ferritin, ferritin light chain, transferrin, beta-2 transferrin and bacterioferritin-based anti-cancer nano drugs encapsulating nanosphere as DNA-binding proteins from starved cells (DPS). Mod Appro Drug Des 1.

188. Heidari A (2017) Potency of human interferon β-1a and human interferon β-1b in enzymotherapy, immunotherapy, chemotherapy, radiotherapy, hormone therapy and targeted therapy of encephalomyelitis disseminate/multiple sclerosis (MS) and hepatitis A, B, C, D, E, F and G virus enter and targets liver cells. J Proteomics Enzymol 6: 1.

189. Heidari A (2017) Transport therapeutic active targeting of human brain tumors enable anti-cancer nanodrugs delivery across the blood-brain barrier (BBB) to treat brain diseases using nanoparticles and nanocarriers under synchrotron radiation. J Pharm Pharm 4: 1-5.

190. Heidari A, Brown C (2017) Combinatorial therapeutic approaches to DNA/RNA and benzylpenicillin (Penicillin G), fluoxetine hydrochloride (prozac and sarafem), propofol (diprivan), acetylsalicylic acid (ASA) (Aspirin), naproxen sodium (aleve and naprosyn) and dextromethamphetamine nanocapsules with surface conjugated DNA/RNA to targeted nano drugs for enhanced anti-cancer efficacy and targeted cancer therapy using nano drugs delivery systems. Ann Adv Chem 1: 061-069.

191. Heidari A (2017) High-resolution simulations of human brain cancer translational nano drugs delivery treatment process under synchrotron radiation. J Transl Res 1: 1-3.

192. Heidari A (2017) Investigation of anti-cancer nano drugs' effects' trend on human pancreas cancer cells and tissues prevention, diagnosis and treatment process under synchrotron and x–ray radiations with the passage of time using mathematica. Curr Trends Anal Bioanal Chem 1: 36-41.

193. Heidari A (2017) Pros and cons controversy on molecular imaging and dynamics of double-standard DNA/RNA of human preserving stem cells-binding nano molecules with androgens/anabolic steroids (AAS) or testosterone derivatives through tracking of helium-4 nucleus (alpha particle) using synchrotron radiation. Arch Biotechnol Biomed 1: 67-100.

194. Heidari A (2017) Visualizing metabolic changes in probing human cancer cells and tissues metabolism using vivo 1H or proton NMR, 13C NMR, 15N NMR and 31P NMR spectroscopy and self-organizing maps under synchrotron radiation. SOJ Mater Sci Eng 5: 1-6.

195. Heidari A (2017) Cavity ring-down spectroscopy (CRDS), circular dichroism spectroscopy, cold vapor atomic fluorescence spectroscopy and correlation spectroscopy comparative study on malignant and benign human cancer cells and tissues with the passage of time under synchrotron radiation. Enliven: Challenges Cancer Detect Ther 4: e001.

196. Heidari A (2017) Laser spectroscopy, laser-induced breakdown spectroscopy and laser-induced plasma spectroscopy comparative study on malignant and benign human cancer cells and tissues with the passage of time under synchrotron radiation. Int J Hepatol Gastroenterol 3: 79-84.

197. Heidari A (2017) Time-resolved spectroscopy and time–stretch spectroscopy comparative study on malignant and benign human cancer cells and tissues with the passage of time under synchrotron radiation. Enliven: Pharmacovigilance and Drug Safety 4: e001.

198. Heidari A (2017) Overview of the role of vitamins in reducing negative effect of decapeptyl (triptorelin acetate or pamoate salts) on prostate cancer cells and tissues in prostate cancer treatment process through transformation of malignant prostate tumors into benign prostate tumors under synchrotron radiation. Open J Anal Bioanal Chem 1: 21-26.

199. Heidari A (2017) Electron phenomenological spectroscopy, electron paramagnetic resonance (EPR) spectroscopy and electron spin resonance (ESR) spectroscopy comparative study on malignant and benign human cancer cells and tissues with the passage

of time under synchrotron radiation. Austin J Anal Pharm Chem 4: 1091.

200. Heidari A (2017) Therapeutic nanomedicine different high-resolution experimental images and computational simulations for human brain cancer cells and tissues using nanocarriers deliver DNA/RNA to brain tumors under synchrotron radiation with the passage of time using mathematica and MATLAB. Madridge J Nano Tech Sci 2: 77-83.

201. Heidari A (2017) A consensus and prospective study on restoring cadmium oxide (CdO) nanoparticles sensitivity in recurrent ovarian cancer by extending the cadmium oxide (CdO) nanoparticles-free interval using synchrotron radiation therapy as antibody-drug conjugate for the treatment of limited–stage small cell diverse epithelial cancers. Cancer Clin Res Rep 1: 2.

202. Heidari A (2017) A novel and modern experimental imaging and spectroscopy comparative study on malignant and benign human cancer cells and tissues with the passage of time under white synchrotron radiation. Cancer Sci Res Open Access 4: 1-8.

203. Heidari A (2017) Different high–resolution simulations of medical, medicinal, clinical, pharmaceutical and therapeutics oncology of human breast cancer translational nano drugs delivery treatment process under synchrotron and x-ray radiations. J Oral Cancer Res 1: 12-17.

204. Heidari A (2017) Vibrational Decihertz (dHz), Centihertz (cHz), Millihertz (mHz), Microhertz (μHz), Nanohertz (nHz), Picohertz (pHz), Femtohertz (fHz), Attohertz (aHz), Zeptohertz (zHz) and Yoctohertz (yHz) imaging and spectroscopy comparative study on malignant and benign human cancer cells and tissues under synchrotron radiation. Int J Biomed 7: 335-340.

205. Heidari A (2017) Force spectroscopy and fluorescence spectroscopy comparative study on malignant and benign human cancer cells and tissues with the passage of time under synchrotron radiation. EC Cancer 2: 239-246.

206. Heidari A (2017) Photoacoustic spectroscopy, photoemission spectroscopy and photothermal spectroscopy comparative study on malignant and benign human cancer cells and tissues with the passage of time under synchrotron radiation. BAOJ Cancer Res Ther 3: 45-52.

207. Heidari A (2017) J-spectroscopy, exchange spectroscopy (EXSY), nuclear overhauser effect spectroscopy (NOESY) and total correlation spectroscopy (TOCSY) comparative study on malignant and benign human cancer cells and tissues under synchrotron radiation. EMS Eng Sci J 1: 6-13.

208. Heidari A (2017) Neutron spin echo spectroscopy and spin noise spectroscopy comparative study on malignant and benign human cancer cells and tissues with the passage of time under synchrotron radiation. Int J Biopharm Sci 1: 103-107.

209. Heidari A (2018) Vibrational Decahertz (daHz), Hectohertz (hHz), Kilohertz (kHz), Megahertz (MHz), Gigahertz (GHz), Terahertz (THz), Petahertz (PHz), Exahertz (EHz), Zettahertz (ZHz) and Yottahertz (YHz) imaging and spectroscopy comparative study on malignant and benign human cancer cells and tissues under synchrotron radiation. Madridge J Anal Sci Instrum 2: 41-46.

210. Heidari A (2018) Two-dimensional infrared correlation spectroscopy, linear two-dimensional infrared spectroscopy and non-linear two-dimensional infrared spectroscopy comparative study on malignant and benign human cancer cells and tissues under synchrotron radiation with the passage of time. J Mater Sci Nanotechnol 6: 101.

211. Heidari A (2018) Fourier transform infrared (FTIR) spectroscopy, near-infrared spectroscopy (NIRS) and mid-infrared spectroscopy (MIRS) comparative study on malignant and benign human cancer cells and tissues under synchrotron radiation with the passage of time. Int J Nanotechnol Nanomed 3: 1-6.

212. Heidari A (2018) Infrared photo dissociation spectroscopy and infrared correlation table spectroscopy comparative study on malignant and benign human cancer cells and tissues under synchrotron radiation with the passage of time. Austin Pharmacol Pharm 3: 1011.

213. Heidari A (2017) Novel and transcendental prevention, diagnosis and treatment strategies for investigation of interaction among human blood cancer cells, tissues, tumors and metastases with synchrotron radiation under anti-cancer nano drugs delivery efficacy using MATLAB modeling and simulation. Madridge J Nov Drug Res 1: 18-24.

214. Heidari A (2018) Comparative study on malignant and benign human cancer cells and tissues with the passage of time under synchrotron radiation. Open Access J Trans Med Res 2: 26-32.

215. Gobato MRR, Gobato R, Heidari A (2018) Planting of Jaboticaba trees for landscape repair of degraded area. Landscape Architecture and Regional Planning 3: 1-9.

216. Heidari A (2018) fluorescence spectroscopy, phosphorescence spectroscopy and luminescence spectroscopy comparative study on malignant and benign human cancer cells and tissues under synchrotron radiation with the passage of time. SM J Clin Med Imaging 4: 1018.

217. Heidari A (2018) Nuclear inelastic scattering spectroscopy (NISS) and nuclear inelastic absorption spectroscopy (NIAS) comparative study on malignant and benign human cancer cells and tissues under synchrotron radiation. Int J Pharm Sci 2: 1-14.

218. Heidari A (2018) X-ray diffraction (XRD), powder x-ray diffraction (PXRD) and energy-dispersive x-ray diffraction (EDXRD) comparative study on malignant and benign human cancer cells and tissues under synchrotron radiation. J Oncol Res 2: 1-14.

219. Heidari A (2018) Correlation two-dimensional nuclear magnetic resonance (NMR) (2D-NMR) (COSY) imaging and spectroscopy comparative study on malignant and benign human cancer cells and tissues under synchrotron radiation. EMS Cancer Sci 1:1-001.

220. Heidari A (2018) Thermal spectroscopy, photothermal spectroscopy, thermal microspectroscopy, photothermal microspectroscopy, thermal macrospectroscopy and photothermal macrospectroscopy comparative study on malignant and benign human cancer cells and tissues with the passage of time under synchrotron radiation. SM J Biometrics Biostat 3: 1024.

221. Heidari A (2018) A modern and comprehensive experimental biospectroscopic comparative study on human common cancers' cells, tissues and tumors before and after synchrotron radiation therapy. Open Acc J Oncol Med 1.

222. Heidari A (2018) Heteronuclear correlation experiments such as heteronuclear single-quantum correlation spectroscopy (HSQC), heteronuclear multiple-quantum correlation spectroscopy (HMQC) and heteronuclear multiple-bond correlation spectroscopy (HMBC) comparative study on malignant and benign human endocrinology and thyroid cancer cells and tissues under synchrotron radiation. J Endocrinol Thyroid Res 3: 555603.

223. Heidari A (2018) Nuclear resonance vibrational spectroscopy (NRVS), nuclear inelastic scattering spectroscopy (NISS), nuclear inelastic absorption spectroscopy (NIAS) and nuclear resonant inelastic x-ray scattering spectroscopy (NRIXSS) comparative study on malignant and benign human cancer cells and tissues under synchrotron radiation. Int J Bioorg Chem Mol Biol 6: 1-5.

224. Heidari A (2018) A novel and modern experimental approach to vibrational circular dichroism spectroscopy and video spectroscopy comparative study on malignant and benign human cancer cells and tissues with the passage of time under white and monochromatic synchrotron radiation. Glob J Endocrinol Metab 1: 514-519.

225. Heidari A (2018) Pros and cons controversy on heteronuclear correlation experiments such as heteronuclear single-quantum correlation spectroscopy (HSQC), heteronuclear multiple-quantum correlation spectroscopy (HMQC) and heteronuclear multiple-bond correlation spectroscopy (HMBC) comparative study on malignant and benign human cancer cells and tissues under synchrotron radiation. EMS Pharm J 1: 2-8.

226. Heidari A (2018) A modern comparative and comprehensive experimental biospectroscopic study on different types of infrared spectroscopy of malignant and benign human cancer cells and tissues with the passage of time under synchrotron radiation. J Anal Mol Tech 3: 8.

227. Heidari A (2018) Investigation of cancer types using synchrotron technology for proton beam therapy: An experimental biospectroscopic comparative study. Eur Mod Stud J 2: 13-29.

228. Heidari A (2018) Saturated spectroscopy and unsaturated spectroscopy comparative study on malignant and benign human cancer cells and tissues with the passage of time under synchrotron radiation. Imaging J Clin Medical Sci 5: 1-7.

229. Heidari A (2018) Small-angle neutron scattering (SANS) and wide-angle x-ray diffraction (WAXD) comparative study on malignant and benign human cancer cells and tissues under synchrotron radiation. Int J Bioorg Chem Mol Biol 6: 1-6.

230. Heidari A (2018) Investigation of bladder cancer, breast cancer, colorectal cancer, endometrial cancer, kidney cancer, leukemia, liver, lung cancer, melanoma, non-Hodgkin lymphoma, pancreatic cancer, prostate cancer, thyroid cancer and non-melanoma skin cancer using synchrotron technology for proton beam therapy: An experimental biospectroscopic comparative study. Ther Res Skin Dis 1.

231. Heidari A (2018) Attenuated total reflectance fourier transform infrared (ATR-FTIR) spectroscopy, micro-attenuated total reflectance fourier transform infrared (micro-ATR-FTIR) spectroscopy and macro-attenuated total reflectance fourier transform infrared (macro-ATR-FTIR) spectroscopy comparative study on malignant and benign human cancer cells and tissues under synchrotron radiation with the passage of time. Int J Chem Papers 2: 1-12.

232. Heidari A (2018) Mössbauer spectroscopy, Mössbauer emission spectroscopy and 57Fe Mössbauer spectroscopy comparative study on malignant and benign human cancer cells and tissues under synchrotron radiation. Acta Sci Cancer Biol 3: 17-20.

233. Heidari A (2018) Comparative study on malignant and benign human cancer cells and tissues under

synchrotron radiation with the passage of time. Org Med Chem IJ 6: 555676.

234. Heidari A (2018) Correlation spectroscopy, exclusive correlation spectroscopy and total correlation spectroscopy comparative study on malignant and benign human AIDS-related cancers cells and tissues with the passage of time under synchrotron radiation. Int J Bioanal Biomed 2: 1-7.

235. Heidari A (2018) Biomedical instrumentation and applications of biospectroscopic methods and techniques in malignant and benign human cancer cells and tissues studies under synchrotron radiation and anti-cancer nano drugs delivery. Am J Nanotechnol Nanomed 1: 1-9.

236. Heidari A (2018) Vivo 1H or Proton NMR, 13C NMR, 15N NMR and 31P nmr spectroscopy comparative study on malignant and benign human cancer cells and tissues under synchrotron radiation. Ann Biomet Biostat 1: 1001.

237. Heidari A (2018) Grazing-incidence small-angle neutron scattering (GISANS) and grazing-incidence x-ray diffraction (GIXD) comparative study on malignant and benign human cancer cells, tissues and tumors under synchrotron radiation. Ann Cardiovasc Surg 1: 1006.

238. Heidari A (2018) Adsorption isotherms and kinetics of multi-walled carbon nanotubes (MWCNTs), boron nitride nanotubes (BNNTs), amorphous boron nitride nanotubes (a-BNNTs) and hexagonal boron nitride nanotubes (h-BNNTs) for eliminating carcinoma, sarcoma, lymphoma, leukemia, germ cell tumor and blastoma cancer cells and tissues. Clin Med Rev Case Rep 5: 201.

239. Heidari A (2018) Correlation spectroscopy (COSY), exclusive correlation spectroscopy (ECOSY), total correlation spectroscopy (TOCSY), incredible natural-abundance double-quantum transfer experiment (INADEQUATE), heteronuclear single-quantum correlation spectroscopy (HSQC), heteronuclear multiple-bond correlation spectroscopy (HMBC), nuclear overhauser effect spectroscopy (NOESY) and rotating frame nuclear overhauser effect spectroscopy (ROESY) comparative study on malignant and benign human cancer cells and tissues under synchrotron radiation. Acta Sci Pharm Sci 2: 30-35.

240. Heidari A (2018) Small-angle x-ray scattering (SAXS), ultra-small angle x-ray scattering (USAXS), fluctuation x-ray scattering (FXS), wide-angle x-ray scattering (WAXS), grazing-incidence small-angle x-ray scattering (GISAXS), grazing-incidence wide-angle x-ray scattering (GIWAXS), small-angle neutron scattering (SANS), grazing-incidence small-angle neutron scattering (GISANS), x-ray diffraction (XRD), powder x-ray diffraction (PXRD), wide-angle x-ray diffraction (WAXD), grazing-incidence x-ray diffraction (GIXD) and energy-dispersive x-ray diffraction (EDXRD) comparative study on malignant and benign human cancer cells and tissues under synchrotron radiation. Oncol Res Rev 1: 1-10.

241. Heidari A (2018) Pump-probe spectroscopy and transient grating spectroscopy comparative study on malignant and benign human cancer cells and tissues with the passage of time under synchrotron radiation. Adv Mater Sci Eng 2: 1-7.

242. Heidari A (2018) Grazing-incidence small-angle x-ray scattering (GISAXS) and grazing-incidence wide-angle x-ray scattering (GIWAXS) comparative study on malignant and benign human cancer cells and tissues under synchrotron radiation. Insights Pharmacol Pharm Sci 1: 1-8.

243. Heidari A (2018) Acoustic spectroscopy, acoustic resonance spectroscopy and auger spectroscopy comparative study on anti-cancer nanodrugs delivery in malignant and benign human cancer cells and tissues with the passage of time under synchrotron radiation. Nanosci Technol 5: 1-9.

244. Heidari A (2018) Niobium, technetium, ruthenium, rhodium, hafnium, rhenium, osmium and iridium ions incorporation into the nano polymeric matrix (NPM) by immersion of the nano polymeric modified electrode (NPME) as molecular enzymes and drug targets for human cancer cells, tissues and tumors treatment under synchrotron and synchrocyclotron radiations. Nanomed Nanotechnol 3: 138.

245. Heidari A (2018) Homonuclear correlation experiments such as homonuclear single-quantum correlation spectroscopy (HSQC), homonuclear multiple-quantum correlation spectroscopy (HMQC) and homonuclear multiple-bond correlation spectroscopy (HMBC) comparative study on malignant and benign human cancer cells and tissues under synchrotron radiation. Austin J Proteomics Bioinform Genomics 5: 1024.

246. Heidari A (2018) Atomic force microscopy based infrared (AFM-IR) spectroscopy and nuclear resonance vibrational spectroscopy comparative study on malignant and benign human cancer cells and tissues under synchrotron radiation with the passage of time. J Appl Biotechnol Bioeng 5: 142-148.

247. Heidari A (2018) Time-dependent vibrational spectral analysis of malignant and benign human cancer cells and tissues under synchrotron radiation. J Cancer Oncol 2: 000124.

248. Heidari A (2018) Palauamine and olympiadane nano molecules incorporation into the nano polymeric matrix

(NPM) by immersion of the nano polymeric modified electrode (NPME) as molecular enzymes and drug targets for human cancer cells, tissues and tumors treatment under synchrotron and synchrocyclotron radiations. Arc Org Inorg Chem Sci 3.

249. Gobato R, Heidari A (2018) Infrared spectrum and sites of action of sanguinarine by molecular mechanics and ab initio methods. Int J Atmosp Ocean Sci 2: 1-9.

250. Heidari A (2018) Angelic acid, diabolic acids, draculin and miraculin nano molecules incorporation into the nano polymeric matrix (NPM) by immersion of the nano polymeric modified electrode (NPME) as molecular enzymes and drug targets for human cancer cells, tissues and tumors treatment under synchrotron and synchrocyclotron radiations. Med Anal Chem Int J 2: 000111.

251. Heidari A (2018) Gamma linolenic methyl ester, 5-Heptadeca-5,8,11-Trienyl 1,3,4-Oxadiazole-2-Thiol, Sulphoquinovosyl Diacyl Glycerol, Ruscogenin, Nocturnoside B, Protodioscine B, Parquisoside-B, Leiocarposide, Narangenin, 7-Methoxy Hespertin, Lupeol, Rosemariquinone, Rosmanol and Rosemadiol nano molecules incorporation into the nano polymeric matrix (NPM) by immersion of the nano polymeric modified electrode (NPME) as molecular enzymes and drug targets for human cancer cells, tissues and tumors treatment under synchrotron and synchrocyclotron radiations. Int J Pharm Anal Acta 2: 7-14.

252. Heidari A (2018) Fourier transform infrared (FTIR) spectroscopy, attenuated total reflectance fourier transform infrared (ATR-TIR) spectroscopy, micro-attenuated total reflectance fourier transform infrared (Micro-ATR-FTIR) spectroscopy, macro-attenuated total reflectance fourier transform infrared (Macro-ATR-FTIR) spectroscopy, two-dimensional infrared correlation spectroscopy, linear two-dimensional infrared spectroscopy, non-linear two-dimensional infrared spectroscopy, atomic force microscopy based infrared (AFM-IR) spectroscopy, infrared photodissociation spectroscopy, infrared correlation table spectroscopy, near-infrared spectroscopy (NIRS), mid-infrared spectroscopy (MIRS), nuclear resonance vibrational spectroscopy, thermal infrared spectroscopy and photothermal infrared spectroscopy comparative study on malignant and benign human cancer cells and tissues under synchrotron radiation with the passage of time. Glob Imaging Insights 3: 1-14.

253. Heidari A (2018) Heteronuclear single-quantum correlation spectroscopy (HSQC) and heteronuclear multiple–bond correlation spectroscopy (HMBC) comparative study on malignant and benign human cancer cells, tissues and tumors under synchrotron and synchrocyclotron radiations. Chro Med Sur 2: 144-156.

254. Heidari A (2018) Tetrakis (3,5-bis (Trifluoromethyl) Phenyl) borate (BARF)-enhanced precatalyst preparation stabilization and initiation (EPPSI) nano molecules. Med Res Clin Case Rep 2: 113-126.

255. Heidari A (2018) Sydnone, münchnone, montréalone, mogone, montelukast, quebecol and palau'amine-enhanced precatalyst preparation stabilization and initiation (EPPSI) nano molecules. Sur Cas Stud Op Acc J 1.

256. Heidari A (2018) Fornacite, orotic acid, rhamnetin, sodium ethyl xanthate (SEX) and spermine (spermidine or polyamine) nanomolecules incorporation into the nanopolymeric matrix (NPM). Int J Biochem Biomol 4: 1-19.

257. Heidari A, Gobato R (2018) Putrescine, cadaverine, spermine and spermidine–enhanced precatalyst preparation stabilization and initiation (EPPSI) nano molecules. Parana J Sci Educ 4: 1-14.

258. Heidari A (2018) Cadaverine (1,5-pentanediamine or pentamethylenediamine), diethyl azodicarboxylate (DEAD or DEADCAT) and putrescine (tetramethylenediamine) nano molecules incorporation into the nano polymeric matrix (NPM) by immersion of the nano polymeric modified electrode (NPME) as molecular enzymes and drug targets for human cancer cells, tissues and tumors treatment under synchrotron and synchrocyclotron radiations. HIV Sex Health Open Access Open J 1: 4-11.

259. Heidari A (2018) Improving the performance of nano-endofullerenes in polyaniline nanostructure-based biosensors by covering californium colloidal nanoparticles with multi-walled carbon nanotubes. J Adv Nanomater 3: 1-28.

260. Gobato R, Heidari A (2018) Molecular mechanics and quantum chemical study on sites of action of sanguinarine using vibrational spectroscopy based on molecular mechanics and quantum chemical calculations. Malay J Chem 20: 1-23.

261. Heidari A (2018) Vibrational biospectroscopic studies on anti–cancer nanopharmaceuticals (Part I). Malay J Chem 20: 33-73.

262. Heidari A (2018) Vibrational biospectroscopic studies on anti–cancer nanopharmaceuticals (Part II). Malay J Chem 20: 74-117.

263. Heidari A (2018) Uranocene (U(C8H8)2) and bis(cyclooctatetraene) iron (Fe(C8H8)2 or Fe(COT)2)-enhanced precatalyst preparation stabilization and initiation (EPPSI) nano molecules. Chem Rep 1: 1-16.

264. Heidari A (2018) Biomedical systematic and emerging technological study on human malignant and benign

cancer cells and tissues biospectroscopic analysis under synchrotron radiation. Glob Imaging Insights 3: 1-7.

265. Heidari A (2018) Deep-level transient spectroscopy and x–ray photoelectron spectroscopy (XPS) comparative study on malignant and benign human cancer cells and tissues with the passage of time under synchrotron radiation. Res Dev Mater Sci 7.

266. Heidari A (2018) C70-carboxyfullerenes nano molecules incorporation into the nano polymeric matrix (NPM) by immersion of the nano polymeric modified electrode (NPME) as molecular enzymes and drug targets for human cancer cells, tissues and tumors treatment under synchrotron and synchrocyclotron radiations. Glob Imaging Insights 3: 1-7.

267. Heidari A (2018) The effect of temperature on cadmium oxide (CdO) nanoparticles produced by synchrotron radiation in the human cancer cells, tissues and tumors. Int J Adv Chem 6: 140-156.

268. Heidari A (2018) A clinical and molecular pathology investigation of correlation spectroscopy (COSY), exclusive correlation spectroscopy (ECOSY), total correlation spectroscopy (TOCSY), heteronuclear single-quantum correlation spectroscopy (HSQC) and heteronuclear multiple-bond correlation spectroscopy (HMBC) comparative study on malignant and benign human cancer cells, tissues and tumors under synchrotron and synchrocyclotron radiations using cyclotron versus synchrotron, synchrocyclotron and the large hadron collider (LHC) for delivery of proton and helium ion (charged particle) beams for oncology radiotherapy. Eur J Adv Eng Technol 5: 414-426.

269. Heidari A (2018) Nano molecules incorporation into the nano polymeric matrix (NPM) by immersion of the nano polymeric modified electrode (NPME) as molecular enzymes and drug targets for human cancer cells, tissues and tumors treatment under synchrotron and synchrocyclotron radiations. J Oncol Res 1: 1-20.

270. Heidari A (2018) Use of molecular enzymes in the treatment of chronic disorders. Canc Oncol Open Access J 1: 12-15.

271. Heidari A (2018) Vibrational biospectroscopic study and chemical structure analysis of unsaturated polyamides nanoparticles as anti-cancer polymeric nanomedicines using synchrotron radiation. Int J Adv Chem 6: 167-189.

272. Heidari A (2018) Adamantane, irene, naftazone and pyridine-enhanced precatalyst preparation stabilization and initiation (PEPPSI) nano molecules. Madridge J Nov Drug Res 2: 61-67.

273. Heidari A (2018) Heteronuclear single-quantum correlation spectroscopy (HSQC) and heteronuclear multiple-bond correlation spectroscopy (HMBC) comparative study on malignant and benign human cancer cells and tissues with the passage of time under synchrotron radiation. Madridge J Nov Drug Res 2: 68-74.

274. Heidari A, Gobato R (2018) A novel approach to reduce toxicities and to improve bioavailabilities of DNA/RNA of human cancer cells-containing cocaine (Coke), lysergide (Lysergic Acid Diethyl Amide or LSD), Δ⁹-Tetrahydrocannabinol (THC) [(–)–trans–Δ⁹–Tetrahydrocannabinol], Theobromine (Xantheose), Caffeine, Aspartame (APM) (NutraSweet) and Zidovudine (ZDV) [Azidothymidine (AZT)] as anti-cancer nano drugs by co-assembly of dual anti-cancer nano drugs to inhibit DNA/RNA of human cancer cells drug resistance. Parana J Sci Educ 4: 1-17.

275. Heidari A, Gobato R (2018) Ultraviolet photoelectron spectroscopy (UPS) and ultraviolet-visible (UV-Vis) spectroscopy comparative study on malignant and benign human cancer cells and tissues with the passage of time under synchrotron radiation. Parana J Sci Educ 4: 18-33.

276. Gobato R, Heidari A, Mitra A (2018) The creation of C13H20BeLi2SeSi. The proposal of a bio-inorganic molecule, using ab initio methods for the genesis of a nano membrane. Arc Org Inorg Chem Sci 3.

277. Gobato R, Heidari A (2018) Using the quantum chemistry for genesis of a nano biomembrane with a combination of the elements Be, Li, Se, Si, C and H. J Nanomed Res7: 241-252.

278. Heidari A (2018) Bastadins and bastaranes-enhanced precatalyst preparation stabilization and initiation (EPPSI) nano molecules. Glob Imaging Insights 3: 1-7.

279. Heidari A (2018) Fucitol, pterodactyladiene, DEAD or DEADCAT (DiEthyl AzoDiCArboxylaTe), skatole, the nanoputians, thebacon, pikachurin, tie fighter, spermidine and mirasorvone nano molecules incorporation into the nano polymeric matrix (NPM) by immersion of the nano polymeric modified electrode (NPME) as molecular enzymes and drug targets for human cancer cells, tissues and tumors treatment under synchrotron and synchrocyclotron radiations. Glob Imaging Insights 3: 1-8.

280. Dadvar E, Heidari A (2018) A review on separation techniques of graphene oxide (GO)/base on hybrid polymer membranes for eradication of dyes and oil compounds: Recent progress in graphene oxide (GO)/base on polymer membranes-related nanotechnologies. Clin Med Rev Case Rep 5: 228.

281. Heidari A, Gobato R (2018) First-time simulation of deoxyuridine monophosphate (dUMP) (Deoxyuridylic Acid or Deoxyuridylate) and vomitoxin

(Deoxynivalenol (DON)) ((3α,7α)–3,7,15–Trihydroxy–12,13–Epoxytrichothec–9–En–8–One)–enhanced precatalyst preparation stabilization and initiation (EPPSI) nano molecules incorporation into the nano polymeric matrix (NPM) by immersion of the nano polymeric modified electrode (NPME) as molecular enzymes and drug targets for human cancer cells, tissues and tumors treatment under synchrotron and synchrocyclotron radiations. Parana J Sci Educ 4: 46-67.

282. Heidari A (2018) Buckminsterfullerene (fullerene), bullvalene, dickite and josiphos ligands nano molecules incorporation into the nano polymeric matrix (NPM) by immersion of the nano polymeric modified electrode (NPME) as molecular enzymes and drug targets for human hematology and thromboembolic diseases prevention, diagnosis and treatment under synchrotron and synchrocyclotron radiations. Glob Imaging Insights 3: 1-7.

283. Heidari A (2018) Fluctuation x-ray scattering (FXS) and wide-angle x-ray scattering (WAXS) comparative study on malignant and benign human cancer cells and tissues under synchrotron radiation. Glob Imaging Insights 3: 1-7.

284. Heidari A (2018) A novel approach to correlation spectroscopy (COSY), exclusive correlation spectroscopy (ECOSY), total correlation spectroscopy (TOCSY), incredible natural-abundance double-quantum transfer experiment (INADEQUATE), heteronuclear single-quantum correlation spectroscopy (HSQC), heteronuclear multiple-bond correlation spectroscopy (HMBC), nuclear overhauser effect spectroscopy (NOESY) and rotating frame nuclear overhauser effect spectroscopy (ROESY) comparative study on malignant and benign human cancer cells and tissues under synchrotron radiation. Glob Imaging Insights 3: 1-9.

285. Heidari A (2018) Terphenyl–based reversible receptor with rhodamine, rhodamine-based molecular probe, rhodamine-based using the spirolactam ring opening, rhodamine b with ferrocene substituent, calix[4]arene-based receptor, thioether + aniline–derived ligand framework linked to a fluorescein platform, mercuryfluor–1 (flourescent probe), N,N'–Dibenzyl–1,4,10,13–Tetraraoxa–7,16–Diazacyclooctadecane and Terphenyl-based reversible receptor with pyrene and quinoline as the fluorophores-enhanced precatalyst preparation stabilization and initiation (EPPSI) nano molecules. Glob Imaging Insights 3: 1- 9.

286. Heidari A (2018) Small-angle x-ray scattering (SAXS), Ultra-small angle x-ray scattering (USAXS), fluctuation x-ray scattering (FXS), wide-angle x-ray scattering (WAXS), grazing-Incidence Small-Angle X-Ray Scattering (GISAXS), grazing-incidence wide-angle x-ray scattering (GIWAXS), small-angle neutron scattering (SANS), grazing-incidence small-angle neutron scattering (GISANS), x-ray diffraction (XRD), powder x-ray diffraction (PXRD), wide-angle x-ray diffraction (WAXD), grazing-incidence x-ray diffraction (GIXD) and energy-dispersive x-ray diffraction (EDXRD) comparative study on malignant and benign human cancer cells and tissues under synchrotron radiation. Glob Imaging Insights 3: 1-10.

287. Heidari A (2018) Nuclear resonant inelastic x-ray scattering spectroscopy (NRIXSS) and nuclear resonance vibrational spectroscopy (NRVS) comparative study on malignant and benign human cancer cells and tissues under synchrotron radiation. Glob Imaging Insights 3: 1-7.

288. Heidari A (2018) Small-angle x-ray scattering (SAXS) and ultra-small angle x-ray scattering (USAXS) comparative study on malignant and benign human cancer cells and tissues under synchrotron radiation. Glob Imaging Insights 3: 1-7.

289. Heidari A (2018) Curious chloride (CmCl3) and titanic chloride (TiCl4)-enhanced precatalyst preparation stabilization and initiation (EPPSI) nano molecules for cancer treatment and cellular therapeutics. J Cancer Res Ther Interv 1: 1-10.

290. Gobato R, Gobato MRR, Heidari A, Mitra A (2018) Spectroscopy and dipole moment of the molecule C13H20BeLi2SeSi via quantum chemistry using ab initio, Hartree-Fock method in the base set CC-pVTZ and 6-311G**(3df, 3pd). Arc Org Inorg Chem Sci 3: 402-409.

291. Heidari A (2018) C60 and C70-encapsulating carbon nanotubes incorporation into the nano polymeric matrix (NPM) by immersion of the nano polymeric modified electrode (NPME) as molecular enzymes and drug targets for human cancer cells, tissues and tumors treatment under synchrotron and synchrocyclotron radiations. Integr Mol Med 5: 1-8.

292. Heidari A (2018) Two-dimensional (2D) 1H or proton NMR, 13C NMR, 15N NMR and 31P NMR spectroscopy comparative study on malignant and benign human cancer cells and tissues under synchrotron radiation with the passage of time. Glob Imaging Insights 3: 1-8.

293. Heidari A (2018) FT-Raman spectroscopy, coherent anti-stokes Raman spectroscopy (CARS) and Raman optical activity spectroscopy (ROAS) comparative study on malignant and benign human cancer cells and tissues with the passage of time under synchrotron radiation. Glob Imaging Insights 3: 1-8.

294. Heidari A (2018) A modern and comprehensive investigation of inelastic electron tunneling spectroscopy (IETS) and scanning tunneling spectroscopy on malignant and benign human cancer cells, tissues and tumors through optimizing synchrotron microbeam radiotherapy for human cancer treatments and diagnostics: An experimental biospectroscopic comparative study. Glob Imaging Insights 3: 1-8.

295. Heidari A (2018) A hypertension approach to thermal infrared spectroscopy and photothermal infrared spectroscopy comparative study on malignant and benign human cancer cells and tissues under synchrotron radiation with the passage of time. Glob Imaging Insights 3: 1-8.

296. Heidari A (2018) Incredible natural-abundance double-quantum transfer experiment (INADEQUATE), nuclear overhauser effect spectroscopy (NOESY) and rotating frame nuclear overhauser effect spectroscopy (ROESY) comparative study on malignant and benign human cancer cells and tissues under synchrotron radiation. Glob Imaging Insights 3: 1-8.

297. Heidari A (2018) 2-Amino-9-((1S, 3R, 4R)-4-Hydroxy-3-(Hydroxymethyl)-2-Methylenecyclopentyl)-1H-Purin-6(9H)-One, 2-Amino-9-((1R, 3R, 4R)-4-Hydroxy-3-(Hydroxymethyl)-2-Methylenecyclopentyl)-1H-Purin-6(9H)-One, 2-Amino-9-((1R, 3R, 4S)- 4-Hydroxy-3-(Hydroxymethyl)-2-Methylenecyclopentyl)-1H-Purin-6(9H)-One and 2-Amino-9-((1S, 3R, 4S)-4-Hydroxy-3-(Hydroxymethyl)-2-Methylenecyclopentyl)-1H-Purin-6(9H)-one-enhanced precatalyst preparation stabilization and initiation nano molecules. Glob Imaging Insights 3: 1-9.

298. Gobato R, Gobato MRR, Heidari A, Mitra A (2018) Spectroscopy and dipole moment of the molecule C13H20BeLi2SeSi via quantum chemistry using ab initio, Hartree-Fock method in the base set CC–pVTZ and 6–311G**(3df, 3pd). Am J Qual Chem Mol Spec 2: 9-17.

299. Heidari A (2018) Production of electrochemiluminescence (ECL) biosensor using Os–Pd/HfC nanocomposites for detecting and tracking of human gastroenterological cancer cells, tissues and tumors. Int J Med Nano Res 5: 22-34.

300. Heidari A (2018) Enhancing the raman scattering for diagnosis and treatment of human cancer cells, tissues and tumors using cadmium oxide (CdO) nanoparticles. J Toxicol Risk Assess 4: 12-25.

301. Heidari A (2018) Human malignant and benign human cancer cells and tissues biospectroscopic analysis under synchrotron radiation using anti-cancer nano drugs delivery. Integr Mol Med 5: 1-13.

302. Heidari A (2018) Analogous nano compounds of the form M(C8H8)2 exist for M=(Nd, Tb, Pu, Pa, Np, Th and Yb)–enhanced precatalyst preparation stabilization and initiation (EPPSI) nano molecules. Integr Mol Med 5: 1-8.

303. Heidari A (2018) Hadron spectroscopy, Baryon spectroscopy and Meson spectroscopy comparative study on malignant and benign human cancer cells and tissues under synchrotron radiation. Integr Mol Med 5: 1-8.

304. Gobato R, Gobato MRR, Heidari A (2019) Raman spectroscopy study of the nano molecule C13H20BeLi2SeSi using ab initio and Hartree-Fock methods in the basis set CC–pVTZ and 6–311G** (3df, 3pd). Int J Adv Eng Sci 7: 14-35.

305. Heidari A, Gobato R (2019) Evaluating the effect of anti-cancer nano drugs dosage and reduced leukemia and polycythemia vera levels on trend of the human blood and bone marrow cancers under synchrotron radiation. Trends Res 2: 1-8.

306. Heidari A, Gobato R (2019) Assessing the variety of synchrotron, synchrocyclotron and LASER radiations and their roles and applications in human cancer cells, tissues and tumors diagnosis and treatment. Trends Res 2: 1-8.

307. Heidari A, Gobat R (2019) Pros and cons controversy on malignant human cancer cells, tissues and tumors transformation process to benign human cancer cells, tissues and tumors. Trends Res 2: 1-8.

308. Heidari A, Gobato R (2019) Three-dimensional (3D) simulations of human cancer cells, tissues and tumors for using in human cancer cells, tissues and tumors diagnosis and treatment as a powerful tool in human cancer cells, tissues and tumors research and anti-cancer nano drugs sensitivity and delivery area discovery and evaluation. Trends Res 2: 1-8.

309. Heidari A, Gobato R (2019) Investigation of energy production by synchrotron, synchrocyclotron and laser radiations in human cancer cells, tissues and tumors and evaluation of their effective on human cancer cells, tissues and tumors treatment trend. Trends Res 2: 1-8.

310. Heidari A, Gobato R (2019) High-resolution mapping of DNA/RNA hypermethylation and hypomethylation process in human cancer cells, tissues and tumors under synchrotron radiation. Trends Res 2: 1-9.

311. Heidari A (2019) A novel and comprehensive study on manufacturing and fabrication nanoparticles methods and techniques for processing cadmium oxide (CdO) nanoparticles colloidal solution. Glob Imaging Insights 4: 1-8.

312. Heidari A (2019) A combined experimental and computational study on the catalytic effect of aluminum nitride nanocrystal (AlN) on the Polymerization of benzene, naphthalene, anthracene, phenanthrene, chrysene and tetracene. Glob Imaging Insights 4: 1-8.

313. Heidari A (2019) Novel experimental and three-dimensional (3D) multiphysics computational framework of Michaelis-Menten kinetics for catalyst processes innovation, characterization and carrier applications. Glob Imaging Insights 4: 1-8.

314. Heidari A (2019) The hydrolysis constants of copper (I) (Cu+) and copper (II) (Cu2+) in aqueous solution as a function of pH using a combination of pH measurement and biospectroscopic methods and techniques. Glob Imaging Insights 4: 1-8.

315. Heidari A (2019) Vibrational biospectroscopic study of ginormous virus-sized macromolecule and polypeptide macromolecule as mega macromolecules using attenuated total reflectance-fourier transform infrared (ATR-FTIR) spectroscopy and mathematica 11.3. Glob Imaging Insights 4: 1-8.

316. Heidari A (2019) Three-dimensional (3D) imaging spectroscopy of carcinoma, sarcoma, leukemia, lymphoma, multiple myeloma, melanoma, brain and spinal cord tumors, germ cell tumors, neuroendocrine tumors and carcinoid tumors under synchrotron radiation. Glob Imaging Insights 4: 1-9.

317. Gobato R, Gobato MRR, Heidari A, Mitra A (2019) New nano-molecule kurumi–C13H 20BeLi2SeSi/C13H19BeLi2SeSi, and Raman spectroscopy using ab initio, Hartree-Fock method in the base set CC–pVTZ and 6–311G** (3df, 3pd). J Anal Pharm Res 8: 1-6.

318. Heidari A, Esposito J, Caissutti A (2019) The importance of attenuated total reflectance fourier transform infrared (ATR-FTIR) and Raman biospectroscopy of single-walled carbon nanotubes (SWCNT) and multi-walled carbon nanotubes (MWCNT) in interpreting infrared and Raman spectra of human cancer cells, tissues and tumors. Oncogen 2: 1-21.

319. Heidari A, Esposito J, Caissutti A (2019) Study of anti-cancer properties of thin layers of cadmium oxide (CdO) nanostructure. Int J Anal Bioanal Methods 1: 20.